# Finite Element Analysis on the Effects of Elastomeric Inclusions for Abating Heat Transfer in Steel Reinforced Concrete Columns

by

Bassam Mohammed Ziadeh

A Thesis Presented in Partial Fulfillment
of the Requirements for the Degree
Master of Science

Approved June 2011 by the
Graduate Supervisory Committee:

Patrick Phelan, Chair
Kamil Kaloush, Co-Chair
Hanqing Jiang

ARIZONA STATE UNIVERSITY

August 2011

# ABSTRACT

Concrete columns constitute the fundamental supports of buildings, bridges, and various other infrastructures, and their failure could lead to the collapse of the entire structure. As such, great effort goes into improving the fire resistance of such columns. In a time sensitive fire situation, a delay in the failure of critical load bearing structures can lead to an increase in time allowed for the evacuation of occupants, recovery of property, and access to the fire.

Much work has been done in improving the structural performance of concrete including reducing column sizes and providing a safer structure. As a result, high–strength (HS) concrete has been developed to fulfill the needs of such improvements. HS concrete varies from normal–strength (NS) concrete in that it has a higher stiffness, lower permeability and larger durability. This, unfortunately, has resulted in poor performance under fire. The lower permeability allows for water vapor to build up causing HS concrete to suffer from explosive spalling under rapid heating. In addition, the coefficient of thermal expansion (CTE) of HS concrete is lower than that of NS concrete.

In this study, the effects of introducing a region of crumb rubber concrete into a steel-reinforced concrete column were analyzed. The inclusion of crumb rubber concrete into a column will greatly increase the thermal resistivity of the overall column, leading to a reduction in core temperature as well as the rate at which the column is heated. Different cases were analyzed while varying the positioning of the crumb-rubber region to characterize the effect of position on the improvement of fire resistance. Computer simulated finite element analysis was

used to calculate the temperature and strain distribution with time across the column's cross-sectional area with specific interest in the steel – concrete region. Of the several cases which were investigated, it was found that the improvement of time before failure ranged between 32 to 45 minutes.

DEDICATION

To my parents, whose endless love, support, and encouragement helped me to achieve so much in this lifeand made me who I am today.

ACKNOWLEDGEMENTS

First and foremost I would like to thank my co-chairs Dr. Patrick Phelan and Dr. Kamil Kaloush. Their guidance and encouragement has enabled the success of this project and help me to overcome many of the challenges I faced. Their willingness to work with me and develop my research to this point has been inspiring. I would also like to thank Dr. Hanqing Jiang for the knowledge I gained from his classes and willingness to help solve the many FEA problems I faced during this work. I would also like to acknowledge Dr. Moudar Zgoul of the University of Jordan for his encouragement throughout my education and for helping develop this project to where it is today.

I would like to express my appreciation to Joseph Shaffer and Anthony Vizzini as well. Their friendship and guidance was been priceless and I could count on them for support on many personal and professional issues. It is because of our numerous discussions and late night cram sessions regarding research and coursework that has allowed me to succeed. Finally, I would like to thank my parents who have always supported me and whose motivation is the reason I have been able to achieve so much. I hope I have made you proud.

TABLE OF CONTENTS

Page

LIST OF TABLES ..... viii

LIST OF FIGURES ..... ix

CHAPTER

1 INTRODUCTION AND PROBLEM STATEMENT ..... 1

1.1 Motivation for Research ..... 1

1.2 Study Objective and Scope of Work ..... 2

1.2.1 Hypothesis ..... 3

1.2.2 Thesis Organization ..... 4

2 LITERATURE REVIEW ..... 7

2.1 Portland Cement Concrete ..... 7

2.2 Recent Developments in Reinforced Concrete ..... 10

2.2.1 Steel Fiber Reinforced Concrete ..... 10

2.2.2 Crumb Rubber Concrete ..... 12

2.3 Crumb Rubber Concrete ..... 15

2.4 Summary ..... 17

3 DETERMINING FAILURE MODE OF SRC COLUMNS IN FIRE 19

3.1 Introduction ..... 19

3.2 Finite Element Analysis in Abaqus ..... 20

3.3 Material Models and Model Assumptions ..... 25

3.4 Fire Failure Mode of a Reinforced Column ..... 31

3.5 Summary ..... 37

4 EFFECTS OF CRUMB RUBBER CONCRETE ON FIRE RESISTANCE OF SRC COLUMNS ..... 39
4.1 Introduction ..... 39
4.2 Analysis Procedure ..... 40
4.3 Material Models ..... 43
4.4 The Effects of an Insulating Crumb Rubber Concrete Region 47
4.4.1 Effects of CRC on Resonant Frequency of Column . 54
4.5 Summary ..... 55
5 EFFECTS OF CRUMB RUBBER CONCRETE ON FIRE RESISTANCE OF SRC COLUMNS ..... 57
5.1 Introduction ..... 57
5.2 Analysis Procedure ..... 59
5.3 The Effects of Crumb Rubber Volume Fraction ..... 60
5.4 Summary ..... 62
6 EFFECTS OF CRUMB RUBBER CONCRETE ON FIRE RESISTANCE OF SRC COLUMNS ..... 63
6.1 Summary of Simulations ..... 63
6.2 Conclusions and Recommendations for Future Work ..... 65
REFERENCES ..... 67
APPENDIX
A MESH CONVERGENCE TEST RESULTS ..... 72
B CONSTITUTIVE SELATIONSHIPS FOR HIGH TEMPERATURE PROPERTIES OF CONCRETE AND STEEL 76

# LIST OF TABLES

Table Page

3.1 Material Properties of Concrete and Steel ..... 28

3.2 Summary of Cases for Characterising SRC Coulm Failure ..... 31

5.1 Test Cases and Failure Times for Various Volume Fractions ..... 60

# LIST OF FIGURES

Figure Page


2.1 Schematic diagram of a wet process kiln used to form clinker, a precursor for Portland cement. ..... 8

2.2 Typical Hooked-End Steel Fiber (dimensions in mm) ..... 11

2.3 Illustration of Mechanism of Spalling of Concrete as a Result of Fire Loading (Courtesy of Zeiml 2006)..... 14

3.1 Figure 3.1 (a) Cross Section of Strandard SRC Concrete Column and (b) FE Model RVE based on a Quarter of the SRC Column (not to scale)..... 27

3.2 A schematic showing (a) the partitioned model and (b) the applied meshing scheme..... 29

3.3 A schematic showing the boundary conditions and applied thermal load as applied in Abaqus. ..... 30

3.4 Temperature of Steel Rebar for Cases #1 – 4 over the Duration of the Simulation ..... 32

3.5 A series of contour plots illustrating strain distribution for Cases #1-4 after 8 hours ..... 33

3.6 Plot of the Max Principal Strain Along Path 1 and 2 for Case #5 and Case #7 after 4 ..... 35

3.7 A series of contour plots illustrating strain distributions for Cases #5 - 7 after 8 ..... 36

3.8 A series of contour plots illustrating difference in strain levels between (a) column confined from expanding at outer edge and (b) column free to expand at outer edge ..... 37

4.1 Finite Element Model of SRC Column with and without CRC region after meshing..... 42

4.2 A series of contour plots illustrating temperature propagation after ~16.5 hours for control and Cases 1-5 ..... 49

4.3 Figure 4.3 Temperature of the steel – concrete interface over the course of the simulation for the Control Case and Cases #1,2 and 5 50

4.4 A series of contour plots illustrating strain distribution after ~16.5 hours for control and Cases 1-5..... 51

4.5 Strain of concrete at steel – concrete interface over the course of the simulation and determination of failure time (inset) ..... 52

4.6 Plot illustrating the increase in failure time for each case study of varying radius of the CRC region ..... 53

4.7 Comparison of first 4 resonant frequencies between the Control Case and Case #5 ..... 55

5.1 A schematic detailing the various volume fractions simulated to assess the effect of volume fraction on fire resistance..... 58

5.2 Strain of concrete at steel – concrete interface over the course of the simulation and determination of failure time (inset) ..... 61

5.3 Improvement in Failure Time for Varying Crumb Rubber Volume Fractions..... 62

A.1 Meshing strategy used for convergence testing using CPE4T elements. ..... 73

A.2 Mesh convergence study for (a) strain at the center of the concrete region with negligible difference between the last two cases and (b) analysis of strain at several temperatures as the mesh is refined. ..... 74

B.1 Modulus of Elasticity of Concrete at High-Temperatures as Utilized for Modeling in this Study ..... 78

B.2 Thermal Conductivity of Concrete at High-Temperatures as Utilized for Modeling in this Study ..... 79

B.3 Thermal Conductivity of Concrete at High-Temperatures as Utilized for Modeling in this Study ..... 80

B.4 Hyperelastic Model of Concrete at High-Temperatures as Utilized for Modeling in this Study ..... 81

B.5 Modulus of Elasticity of Steel at High-Temperatures as Utilized for Modeling in this Study ..... 82

B.6 Thermal Conductivity of Steel at High-Temperatures as Utilized for Modeling in this Study ..... 83

B.7 Specific Heat Capacity of Steel at High-Temperatures as Utilized for Modeling in this Study ..... 84

# Chapter 1

# INTRODUCTION AND PROBLEM STATEMENT

## 1.1 Motivation for Research

Much research in recent years has been geared towards improvements in building safety in light of recent tragedies. There is nothing more tragic than the unnecessary loss of life accompanied with building fires. Because the backbone of major infrastructure, including high-rise buildings, bridges and tunnels, utilize some form of reinforced concrete, many questions regarding their characteristics and performance against fireincidents have risen. Undoubtedly, the invention and integration of reinforced concrete has led to smaller support columns in high-rise buildings, which allows for an increase in useable space, as well as smaller bridge spans, which reduce the overall dead-load the bridge is required to support, and allowing for greater underpass clearance widths (Strong 2004).

Current research has sprung interest into better characterizing and understanding the performance of high strength (HS) concrete in a fire through the use of numerical models (Kodur 2004). These studies have indicated that while HS concrete is a lucrative option due to its improved structural performance, it suffers in a fire situation due to its dense packing and difference in thermal characteristics compared to normal strength concrete.While solutions, such as the inclusion of fiber reinforcements has been shown to improve resistance to spalling (Nataraja, 2000), these solutions do not address the issue of propagating heat within the column and the potential effect on steel reinforcing

rebar. It is well documented that the failure and ultimate collapse of the world trade center towers was a result of the high temperatures that the steel spans and concrete columns experienced due to the burning jet fuel. Other noticeable structural fires included the recent fires in the Channel tunnel, which witnessed explosive spalling from the rapid heating of the concrete in the tunnel. As such there has been great interest in improving the performance of high performance concretes in a fire situation in an attempt to prolong or mitigate such injuries or loss of life.Thus, the issue remains how to decreasethe propagation of heat within the column, which lies in modifying the heat transfer characteristics of a concrete column.

## 1.2 Study Objective and Scope of Work

The objective of this study is to investigate the effects of introducing a region of elastomeric layer into a steel-reinforced concrete column to increase the column's thermal resistivity and reduce its core temperature in case of a fire. The scope of work first includes laying the groundwork for the improvement of the fire resistance of steel reinforced concrete columns; this is done by first gaining an understanding of their primary mode of failure. For which the hypothesis is the rapid expansion of the rebar embedded in the concrete matrix.Next, the incorporationof an insulating layer capable of abating heat propagation within the column in an effort to slow the expansion of the rebar and thus improving the fire resistance of the column is studied. The heat transfer concept will be simulated through the use of finite element analysis (FEA) to support the initial hypothesis and provide an understanding of the mechanism behind the proposed solution.

This section outlines further the objectives and contributions of this work. It will describe the goals of the work and provide a brief outline of each chapter within this thesis.

### 1.2.1 Hypothesis

The concept of fire resistance is well known and well documented. There exist numerous standards that address the testing and design of buildings, such as ASTM E119 and CAN/ULC S101 (Standard Test Methods for Fire Tests of Building Construction and Materials 2000, and Standard Methods of Fire Endurance Tests of Building Construction and Materials 1989). In addition, there has been much work recently to better understand the material properties of HS concrete and steel for use in fires (Youssef 2007, Kodur 2008).

In order to improve their performance in a fire situation, it is understood that little can be done to alter the performance of HS concrete beyond what has been established. Thus, this work will look into incorporating an insulating layer of concrete with elastomeric inclusions into the original reinforced column. This proposed solution will exploit the fact that there are numerous materials with thermal properties that far exceed those of concrete in high temperature situations. There exist many possibilities for such inclusions such as ceramics, which tend to have superior thermal properties but may lack the ability to bond to concrete, or exotic polymers, whose surface and bonding properties could be tweaked to a specific use but tend to be associated with high prices. In this study, the effects of crumb rubber inclusions will be investigated. The characteristics of crumb rubber inclusions in a concrete matrix, commonly referred to as crumb rubber

concrete,have been extensively studied and are relatively well understood (Hernandez-Olivares 2003, Kaloush 2006, Lingannagari 2007). Furthermore, the availability of recycled rubber makes it not only viable from a cost point of view,but an attractive method to recycle rubber in a green and sustainable fashion.

Thus it is proposed in this thesis to incorporate a region of crumb rubber concrete (CRC) into a standard steel reinforced concrete column. It is believed that the addition of a CRC region will decrease heat transfer within the column by using the rubber inclusions to absorb some of the thermal energy within the column. By doing this, the column is expected to heat up at a slower rate, thus improving the fire resistance of the column. The goal of this research work is to lay the foundation and gain insight for utilizing CRC to improve the fire resistance of reinforced columns using numerical simulations.

### 1.2.2 Thesis Organization

Chapter 1 provided a brief introduction to the goal of the research work presented in this thesis. It is postulated that the addition of an insulating layer of CRC to a reinforced concrete column will improve the performance of the column in a fire situation. This will be achieved by exploiting the fact that rubber has superior thermal properties when compared to concrete or steel fibers. The improvement ofthe fire resistance of a column is of importance due to the fact that HS concrete and reinforced concrete columns constitute the primary load bearing supports of many of our infrastructures and their failure could lead to a tragic loss of life and money.

Chapter 2 will introduce the literature review on the main components discussed in this thesis, primarily reinforced concrete columns and crumb rubber concrete. It begins with a brief background on reinforced concrete columns and how they have evolved to the state at which they are at today. This will include the incorporation of steel rebar, steel fibers, and polymer fibers, all of which are used to improve the strength and durability of concrete. In addition, some of the work that has been conducted on the performance of HS concrete and steel in fire situations will be presented. Next, the concept of crumb rubber concrete will be introduced as well as a brief discussion on its current applications and research. Chapter 3 will introduce the concept of fire resistance, how it applies to existing structures and the importance of factoring fire resistance into the design of buildings. In addition, a brief introduction to the concept of finite element (FE) method and how it is implemented in Abaqus will be presented. Several cases will be put forth with the goal of determining the primary cause of failure when steel reinforced concrete columns are exposed to a fire. Chapter 4 investigates the effect a CRC region has on the temperature distribution across the column's cross-section as well as the effect it has on the expansion of steel. Different cases are modeled to establish the position of the CRC region within the column to improve the fire resistance. Chapter 5 provides a brief evaluation into the effect of the amount of rubber, or volume fraction, would have on the improvements found in Chapter 3. The aim of this is to establish a basic understanding of a more applicable case where aggregate size within the concrete would limit or control the amount of crumb rubber within a fixed volume. Chapter 6 provides a

summary of the work. The different models simulated are also summarized along with a brief discussion of their potential applications. Conclusions and recommendations for future work are also included in this chapter.

# Chapter 2

# LITERATURE REVIEW

## 2.1Portland Cement Concrete

In terms of construction materials, Portland Cement concrete (PCC), also simply referred to as “concrete”, is one of the most predominant construction materials in the modern age due to its longevity, durability, and formability. In fact, Birgisson (2010) reports that concrete is the most heavily used construction material in the world, while the Portland Cement Association reports worldwide, 2.310 million metric tons of cement were produced in 2005. The uses of PCC in its many forms can be seen in numerous applications including high-rise buildings, homes, bridges and tunnels, highways and dams (*Handbook of Concrete Technology and Masonry Construction* 1981). Despite this, PCC is rarely used in its virgin state due to challengingproperties such as low tensile strength, relatively low compressive strength (when compared to high-strength concrete), and problems with fire performance. This section will provide background on some of the most important innovations in concrete technology by first explaining the fundamentals of concrete itself in general terms followed by a brief history of concrete technology.

Concrete, by the most basic definition, is a composition of sand, gravel, and crushed rock or aggregate which is held together by a hardening paste of hydraulic cement and water (*Handbook of Concrete Technology and Masonry Construction* 1981). One of the fundamental components of concrete is the

cement paste, of which Portland cement is used to form Portland cement concrete (PCC). Portland cement begins by the heating of a mixture of limestone and clay to a sintering temperature of 1450˚C (Taylor 1990). At this heat, partial fusion occurs and lumps or nodules of clinker are produced; this process is illustrated in Figure 2.1. Clinker is by definition the byproduct of the sintering process. The clinker is then ground into a fine power along with gypsum to form Portland cement. The cement is then mixed with sand, gravel and other aggregates as well as with water, which reacts with the anhydrous concrete to begin the setting and hardening process. As the concrete hydrates, it begins to set and harden as well as bond with the aggregates to form concrete. These aggregates can range from fine aggregates such as sand or gravels to coarse aggregates such as ground rock. The hydration process of cement, particularly Portland cement, is complex and is outside the scope of this thesis, but is covered in great detail in Taylor (1990), Gani (1997) and Hewlett (1998).

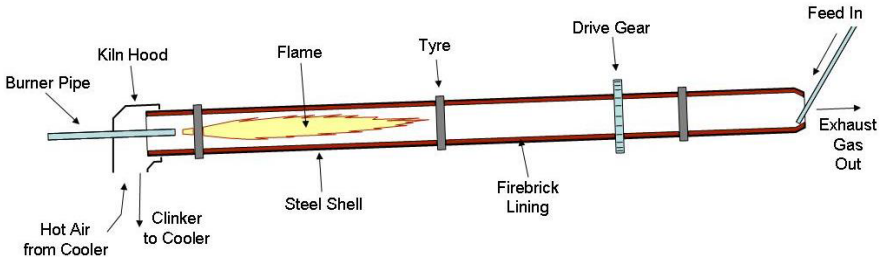


**Figure 2.1 Schematic diagram of a wet process kiln used to form clinker, a precursor for Portland cement. (*Public Domain* courtesy of Wikipedia, Inc)**

While the use of concrete is wide spread today, the use of concrete can actually be traced back to the Roman civilizations, dating back to 7000 BC (Malinowski and Garfinkel 1991), in which the concrete was limestone based as

well as gypsum based concrete used by the Egyptians dating back to 2500 BC (Lea 1970). Despite their long history, the quality of the concrete was poor and inconsistent due to the variation of the properties of the cement and aggregates. It wasn't until 1818 where calcification of limestone and clay was first tried and credited as the forerunner of Portland cement (Gani 1997). It took another six years before Portland cement was formally invented and patented by Joseph Aspdin (Jo 2007, Velez 2008). This form of Portland cement became the standard concrete for much of Europe as well as America in later years.

The modern, high-temperature process of making Portland cement was discovered in 1884 by Issac Johnson. His process brought about concrete production with more reliable strength and setting properties. With the onset of modern Portland cement, the majority of concrete applications by the late 1800s contained this cement. Through its widespread use, one major downfall of concrete was itsrelatively low tensile strength. In order to mitigate this, steel bars, or rebar, are embedded into the concrete matrix to improve the tensile strength. This is often referred to as steel reinforced concrete.

In the early years, it was common to produce concrete with a compressive strength of 20-30 MPa. Recent development resulted in concrete with compressive strengths in the range of 90-110 MPa, and they belong to a class of concrete known as high-strength concrete. The American Concrete Institute (ACI) classifies all concrete up to 42 MPa as *normal-strength concrete* whereas anything above this level in considered to be *high-strength concrete*. In fact, concrete used in current high-rise buildings have a compressive strength of 140

MPa (Nawy 2001). The introduction of high strength concrete not only brought about an age of higher strength concrete, but also improvements to durability and workability (Kodur 2004).

## 2.2Recent Developments in Reinforced Concrete

The first recorded use of reinforced concrete was reported by Kirby (1956) in which he describes how the Romans utilized reinforced concrete to construct a bridge across the Risorgimento River in a single span, although the formal use of reinforced concrete was first patented by Wilkinson in 1855 (Krishna 2007). Ever since the introduction of steel reinforced concrete, numerous other methods have been investigated in order to further improve upon a number of properties. These include the use of steel rebar, steel fibers, and polymer fibers.

### 2.2.1Steel Fiber Reinforced Concrete

From early on, the use of steel fibers (Figure 2.2) has been investigated as a possible reinforcement in concrete. This entails the use of a steel mesh, of varying size, and embedding it into the concrete matrix. Improvements in compressive strength have been documented to range from negligible up to 25% (Balaguru and Shah 1992). This range of improvement has led to its use in highways, pavements, and tunnel linings but interest in using steel-fiber reinforced concrete (SFRC) in structural applications has been suggested by ACI committee 544. Thus, to lay the groundwork for such applications, Nataraja (1999) determined the properties and stress-strain curves for SFRC under compression and found an increase in toughness, compressive strength and peak strain.

Much of the research surrounding steel reinforced concrete (SRC) concerns improving the life and durability of SRC columns, especially in corrosive environments. Of the main concerns facing steel reinforced concrete columns is their structural degradation due to bond degradation at the steel – concrete interface. Among the chief causes of bond strength reduction is the formation of rust, or corrosion of the steel at the steel – concrete interface. A study by Almusallam (1995) found that while a low percent of rust (up to 4%) improved the bond strength due to an increase in surface roughness, an increased amount of corrosion caused a decrease in bond strength.

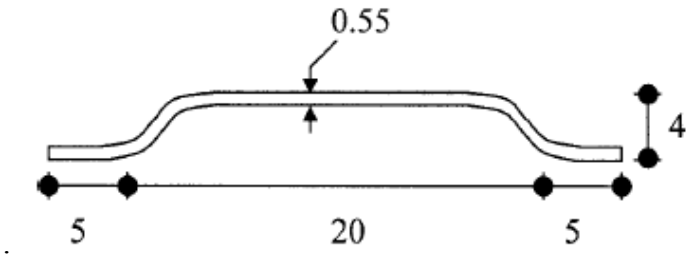


**Figure 2.2 Typical Hooked-End Steel Fiber (dimensions in mm) (Courtesy of Thomas and Ramaswamy 2007)**

To better quantify the improvements seen through the introduction of steel fibers (Figure 2.2), Thomas and Ramaswamy (2007) performed extensive work to quantify the improvements. It was found that through a range of grades (35, 65 and 85 MPa), the steel fibers had little effect on the compressive properties of concrete but its tensile strength witnessed an increase of 40%. In addition the peak compressive strain increased by 30%. These improvements can be attributed to the dispersion of the fibers over the entire matrix and the ability to transfer load over a larger number of specimens.

More current research has investigated the performance of SFRC columns in a fire. Sideris (2009) investigated the effect of steel fibers in high strength concrete to measure their effect on spalling as well as in the loss of compressive strength in high strength concrete. It was found that the steel fibers did not prevent spalling, although the inclusion of steel fibers increased the temperature at which spalling occurs, but decreased the amount of compressive strength loss. Colombo (2010) recently performed an in depth study on the performance of SFRC columns exposed to high temperatures for cases of uniaxial compression, uniaxial tension and bending. It was found that, for a range of temperature, the pull-out of the fibers is less affected by elevated temperatures thus improving the post-cracking behavior of the concrete. For compression testing, it was found that the fibers did not greatly affect the properties of the column while under tension and bending, improvements to the column's ductility were seen over 400˚C.

### 2.2.2 Polymer and Polymer Fiber Reinforced Concrete

In order to further improve the characteristics of concrete, much research has been conducted in the field of using polymer additives into the concrete. While the use of polymer additives, in some form, can be traced to many years earlier; the first apparent use of polymers in PCC was in 1909 in the United States. Since then, much work has been done in developing polymer-modified concrete (PMC), with much of the work done utilizing thermosetting and thermoplastic polymers (Su 1995) and their use for polymer fiber reinforcement. Safi (1999) investigated the use of fiber reinforced polymer (FRP) tubes to improve a wide range of properties, including as a protective jacket for a column

and for shear and flexural reinforcement. It was found that the use of these tubes improved the strength and ductility of the column over SFRC. Li (2003) built on the use of FRP reinforcements to model their behavior under eccentric loading. It was found that due to the creation of bending moments, as well as compressive forces, the improvements of FRP reinforcements are not on the same scale as those seen in pure concentric bending and are in fact negligible.

Interest in the performance of polymer fibers to enhance the performance of columns exposed to fire was reported by Bisby (2005). Bisby investigated the effects of a polymer confined concrete column through numerical models. It was found that while fiber reinforcements improve the structural properties of columns, once exposed to a fire, the polymer degrades and provides very little improvement to the fire resistance of the column. In an effort to build on this effort, Zeiml (2006) investigated the use of polypropylene (PP) fibers embedded within the concrete matrix, as opposed to confining the concrete, in an effort to improve the spalling behavior of concrete in a fire. The hypothesis is that the PP will provide channels for the built up water vapor to escape, thus decreasing the likelihood of spalling. It was showed that the inclusion of 1.5 kg/m$^3$ of PP fibers effectively improved the porosity of the concrete and decreased the likelihood of spalling. The mechanism behind spalling is illustrated in Figure 2.3 and discussed in later chapters.

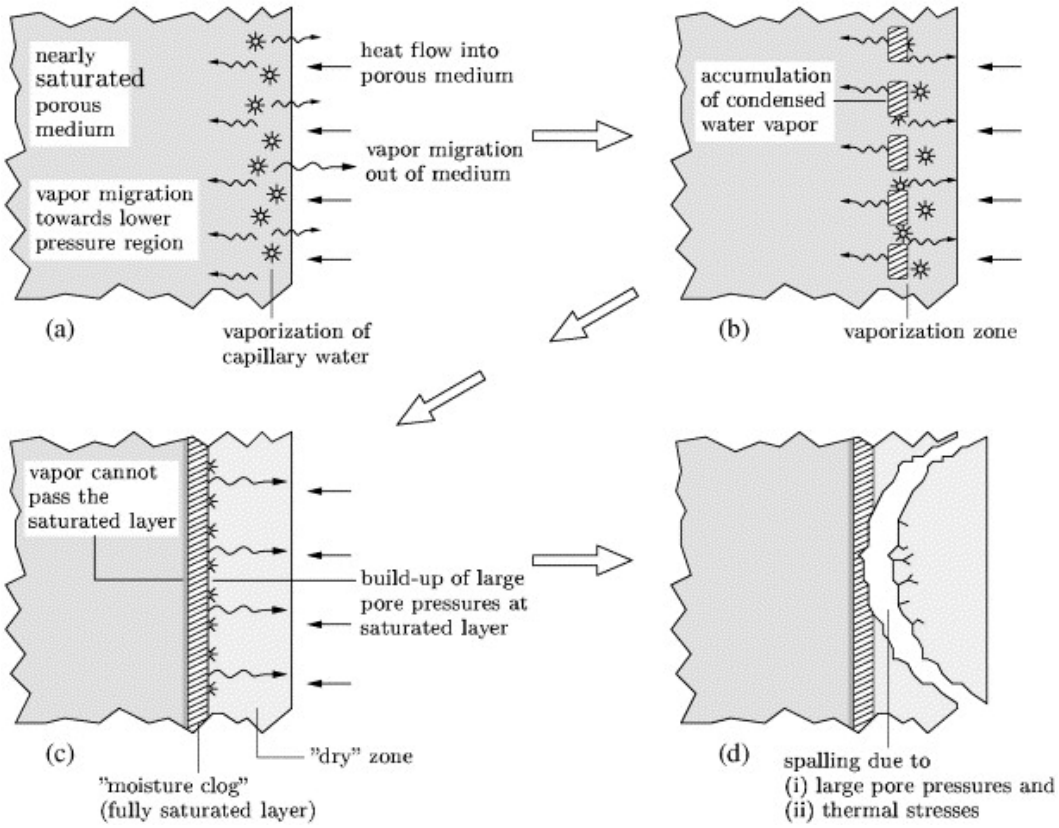


**Figure 2.3 Illustration of Mechanism of Spalling of Concrete as a Result of Fire Loading (Courtesy of Zeiml 2006)**

Peng (2006) built on the idea of using polymer fibers to increase the properties of columns in a fire situation. Peng investigated the mechanical properties of FRP concrete after a fire and found that the fracture energy was significantly higher than standard concrete but for densely packed concrete (high performance concrete), spalling remained an issue. This is due to the high water content and the inability to remove enough pressure to prevent spalling completely. It should be noted that while PP fibers did not completely prevent spalling from occurring, FRP concrete experienced spalling at a later stage. Thus, their inclusion effectively prolonged the onset of spalling. In an effort to further improve on the fire performance of columns, Xiangjun (2008) investigated a form

of hybrid fiber reinforcement by utilizing both steel and polymer fibers. The motivation for this was to negate the negative effect of PP fibers on the strength of HS concrete while maintaining their benefits for spalling. It was found that in this case, spalling under fire was eliminated and the mechanical properties of the column after exposure to fire were improved effectively. While these methods show vast improvements in the performance of pure concrete, none seem to address the issue of the failure of steel rebar reinforced concrete and their potential mode of failure.

## 2.3 Crumb Rubber Concrete

For years the world has struggled with the issue of discarded automobile tires. An estimated 1.2 billion tires were consumed in the United States in 2004. Their disposal brings about another problem, which is typically dealt with by storing in landfills and incineration which tends to release toxic compounds into the environment (Zaharia 2009). Since the 1990s, the State of Arizona has declared the recycling of tires a high priority and as such the Arizona Department of Transportation (ADOT) has supported the use of recycled rubber in numerous applications. Early work by Eldin (1993) investigated the use of recycled rubber particles as an aggregate in concrete. The study focused on the effect of the rubber inclusions on the strength and toughness of Portland cement concrete. It was found that the concrete lost up to 85% of its 28-day compressive strength when 75% of the standard course aggregate was replaced with crumb rubber. It was also found that concrete with rubber aggregate was able to absorb increased plastic energy as well as a shift in failure mode was observed. Toutanji (1994) expanded

on this study by further studying the effects of crumb rubber incorporated as an aggregate in Type II Portland concrete. Similar results were noticed that the compressive strength decreased while the fracture toughness increased significantly. It was also observed that the failure of a crumb rubber concrete column was ductile in nature instead of the traditional brittle fracture. It has thus been suggested that crumb rubber concrete (CRC) be used in non-structural applications, such as pavements (asphalt and concrete) and sidewalks.

In order to increase the possible applications of crumb rubber concrete, Raghavan (1998) further investigated the workability and stability of CRC. While effects on strength were in line with previous studies, it was found that the use of rubber shreds improved the post-fracture characteristics of the concrete. This was due to the fact that the shreds held the two fractured specimens together and continued to carry stress beyond matrix cracking. Furthermore, after long exposure to a high-alkaline environment, the rubber showed less than a 20% reduction in stress value, which would suggest that CRC would not significantly age or degrade. Hernandez-Olivares (2002) built on the expanding interest of the numerous uses of CRC by evaluating the dynamic response of CRC. This is crucial in understanding and providing cheaper damping solutions for structural applications. The study focused on a low volume fraction of 5% rubber particles and found that at such a low volume fraction both static and dynamic properties did not vary from standard concrete. While this may not be significant for damping applications, it has been established that at low volume fractions, CRC could be a viable alternative for standard concrete applications.

In recent years the State of Arizona and ADOT showed increased interest in the use of crumb rubber concrete. Kaloush (2005) and Lingannagari (2007) took part in quantitatively characterizing the mechanical properties of CRC. This study included the physical application of CRC in a number of civil infrastructures around Arizona, including at Arizona State University. The studies found that CRC exhibited a lower coefficient of thermal expansion (CTE) than standard concrete, making it a viable option for environments that experience large thermal cycling. It was also found that while testing, the CRC samples never shattered, thus implying that they may be beneficial in applications where impact is crucial.

Another field of interest, which is also the focus of this thesis, is the use of CRC to improve the fire performance of concrete columns. Little work has been done in this up to date. Hernandez-Olivares (2003) investigated the performance of CRC in a fire, with a focus on studying the stiffness and spalling behavior. It was found that the inclusion of rubber particles reduced the stiffness of high-performance concrete, thus making it more compatible with other materials when ductility is of concern. The fire tests also showed a reduction in curvature and the risk of spalling. While this study is a great starting point, it does not address the effects of fire on a steel rebar reinforced concrete not does it address the issue of temperature propagation.

## 2.4 Summary

Significant work has been conducted in the field of reinforced concrete in an effort to improve the mechanical performance of both normal and high strength

concrete. Methods such as the incorporation of steel fibers showed an improvement in tensile strength. This was attributed to the ability of concrete to chemically bond to steel and effectively transfer tensile load to the fibers. The use of a polymer mesh was also investigated to improve the performance of concrete in terms of its fire performance and structural properties. It was seen that the use of polymer mesh to confine the column resulted in improvements to both tensile and compressive strengths. These confinements, though, did not provide any benefits in a fire application due to their low degradation temperatures. Thus, the use of PP fibers embedded into the concrete was investigated in an effort to improve fire performance. The inclusion of fibers successfully reduced the likelihood of spalling due to their ability to create channels for the water vapor to "escape" through. The inclusions of other polymers, such as rubber, were also investigated. It showed that while at high volume fractions, the mechanical properties suffered, their use in low volume fractions (<5%) showed an improvement to the spalling and little effect on the mechanical properties of concrete. However, the majority of the studies pertaining to fire resistance focused on the reduction of the effect of spalling rather than preventing any failure of the column, specifically in steel rebar reinforced columns. Thus it is critical to develop an innovative approach that blunts the temperature propagation within the column in an effort to improve the fire resistance of the column as well as reduce the effect of spalling.

# Chapter 3

# DETERMINING FAILURE MODE OF SRC COLUMNS IN FIRE

## 3.1 Introduction

Building fires often lead tothe most painful tragedies, in which human lives and valuable property and assets are lost in a relativelyshort time. Any time period gained in prolonging the time before the building collapses may be crucial in saving human lives. The time required for a building to collapse during a fire is an indication of the building's ability to resist failure due to thermal effects. In light of the fact that columns are the building's main support, delaying a columns' failure directly leads to delaying the collapse of the building itself. Therefore, delaying of columns' failure is a reliable factor for improving the building's fire resistance.

High temperatures have a more drastic effect on load bearing columns than the effect of mechanical forces themselves. The effect of high temperature on structures comes in twofold; it drastically degrades the material properties, and secondly, as a result of the degraded material properties, decreases the column's load carrying capacity. Collapse of a column finally occurs when the column's load carrying capacity drops below the load acting on the column.

Fire resistance of a reinforced concrete column depends primarily on the type of aggregate, dimensions of various parts comprising the column, temperature distribution over the column's cross section with time, and the cover of the concrete over the reinforcement. The time required for a building, or

column, to collapse during a fire is an indication of the building's ability to resist failure due to thermal effects (Neves 2002, Reynolds 2008), or more informally the time before failure is the column's *fire resistance*. Furthermore, with increasing fire temperature, the column's temperature will increase quicker and thus the column's carrying capacity will decrease.

In this chapter, the performance of steel reinforced concrete (SRC) columns in a fire scenario is evaluated. Failure time for a column is assessed for different cases through the variation of the fire temperatures,as well as steel rebar location within the column.

## 3.2 Finite Element Analysis in Abaqus

The finite element method, or more commonly termed finite element analysis (FEA), is a numerical technique for finding approximate solutions to partial differential equationsapplicable to engineering problems for which closed form solutions do not exist. Although FEA is typically applied to the fields of structural engineering and heat transfer (MacNeal 1995), it has been adapted to various other fields such as fluid dynamics and electromagnetics.

The basic idea of the FEA method is to divide the structure into finite elements and then a series of equations are solved for each element, rather than for the entire structure, to determine displacements of each element. For any structural problem, regardless of loading or material properties, there are three main conditions that must be satisfied: equilibrium, compatibility, and the Stress-strain law (*NAFEMS A Finite Element Primer* 1992). The degree of complexity experienced in FEM, and the amount of computational power required to solve

the associated equations rests on, among others, the type of element used, the degree of the model (1-D, 2-D or 3-D) as well as the type of load and boundary conditions.

The analysis in this research study uses Abaqus, a SIMULIA product, which is among one of numerous FEA packages available. Abaqus is well known for its ability to incorporate complex material models into various forms of analysis, both static and transient, as well as numerous forms of coupled analysis including coupled temperature – displacement analysis, which will be employed in this research.

Abaqus uses numerical techniques to integrate quantities over the element's volume, which allows it to solve a given problem without depending on its material behavior (Abaqus Analysis User's Manual 2010). Using the displacement-based finite element formulation, Abaqus satisfies the equilibrium condition in its "weak form" by utilizing the principle of virtual work,

$$\int_V \boldsymbol{\sigma} : \delta\boldsymbol{\varepsilon}\, dV = \int_S \mathbf{t} \cdot \delta\mathbf{v}\, dS + \int_V \mathbf{f} \cdot \delta\mathbf{v}\, dV \tag{3.1}$$

where $\boldsymbol{\sigma}$ and $\boldsymbol{\varepsilon}$ and the material stress and strain measures, $\delta\boldsymbol{\varepsilon}$ is the measure of virtual strain rate, $\mathbf{t}$is the surface traction, $\mathbf{f}$ is the body forces, and $\delta\mathbf{v}$ is the virtual work displacement field. The measure of strain used in the analysis and solution is dependent on the type of element used to mesh the structure (Abaqus Theory Manual 2010). In the following simulations, plane strain elements are used. The next step is to select an interpolating function, which is used to describe the behavior of the element,

$$\mathbf{v}(x,t) = N(x)\mathbf{q}(t) \tag{3.2}$$

where N(x) is the shape function and **q**(t) is the vector containing the nodal degrees of freedom. This vector, **q**(t),which contains the degrees of freedom, such as the displacement, rotations and temperature of the nodes must also satisfy the prescribed boundary conditions.

Next, the strain is related to the nodal displacements through the interpolation assumption,

$$\boldsymbol{\varepsilon}(x,t) = B(x)\mathbf{q}(t) \tag{3.3}$$

where B(x) is a function of the geometry and the shape function N(x). The constitutive relation is then satisfied according to,

$$\boldsymbol{\sigma}(x,t) = D\boldsymbol{\varepsilon}(x,t) \tag{3.4}$$

where D is a positive definite matrix. Continuing, if we substitute equation (3.2) through (3.4) into equation (3.1) and neglecting any applied body forces eventually yields a system of equations in the form,

$$\mathbf{Kq} = \mathbf{F}; \tag{3.5}$$

where

$$\mathbf{K} = \int_V \mathbf{B}^T\mathbf{DB}dV,$$
$$\mathbf{F} = \int_A N^T \cdot \mathbf{t}dA$$

where **K** is typically referred to as the stiffness matrix and **F** is the applied force.

In addition to solving the weak form to solve structural problems, this research also utilizes Abaqus' capability to solve heat transfer problems to model solid body heat conduction. This is done utilizing general, temperature-dependent

conductivity, internal energy effects, and general convection and radiation boundary conditions. Abaqus satisfies the equilibrium condition in its "weak form" by solving the basic energy balance,

$$\int_V \rho \dot{U}\, dV = \int_S q dS + \int_V r dV \tag{3.6}$$

where V is the volume of the solid material, with surface area S; ρ is the density of the material, $\dot{U}$ is the material time rate of the internal energy; q is the heat flux per unit area; and r is the external heat supplied per unit volume. It is then assumed that U = U(θ), where θ is the temperature of the material thus it is written in terms of specific heat,

$$c(\theta) = \frac{dU}{d\theta} \tag{3.7}$$

Heat conduction is then calculated and is assumed to be governed by the Fourier Law,

$$\mathbf{f} = -\mathbf{k}\frac{d\theta}{d\mathbf{x}} \tag{3.8}$$

where **k** is the conductivity matrix; f is the heat flux; and **x** is the position. A variation of the energy balance equation is obtained by the Galerkin method by combining equations (3.6) and (3.8),

$$\int_V \rho \dot{U}\, \delta\theta dV + \int_V \frac{\partial \delta\theta}{\partial \mathbf{x}} \cdot \mathbf{k} \cdot \frac{\partial \theta}{\partial \mathbf{x}} = \int_V \delta\theta r dV + \int_{sq} \delta\theta q dS \tag{3.9}$$

where δθ is an arbitrary variational field satisfying the essential boundary conditions. The body is then segmented into finite elements and the body temperature is interpolated by,

$$\theta = N^N(\mathbf{x})\theta^N, N = 1,2,..., \tag{3.10}$$

where $\theta^N$ are nodal temperatures and N are first and second order polynomial shape functions as described previously. Furthermore the Galerkin approach assumes that δθ interpolated by the same functions,

$$\delta\theta = N^N\delta\theta^N \tag{3.11}$$

Combining the interpolations of (3.10) and (3.11) into (3.9), it becomes,

$$\delta\theta^N\left(\int_V N^N\rho\dot{U}\,dV + \int_V \frac{\partial N^N}{\partial \mathbf{x}}\cdot\mathbf{k}\cdot\frac{\partial\theta}{\partial\mathbf{x}}\,dV = \int_V N^N r dV + \int_{Sq} N^N q dS\right) \tag{3.12}$$

and since $\delta\theta^N$ is chosen arbitrarily, this gives the system of equations,

$$\int_V N^N\rho\dot{U}\,dV + \int_V \frac{\partial N^N}{\partial \mathbf{x}}\cdot\mathbf{k}\cdot\frac{\partial\theta}{\partial\mathbf{x}}\,dV = \int_V N^N r dV + \int_{Sq} N^N q dS \tag{3.14}$$

This set of equations is the "continuous time description" of the geometric approximation generated after the body is discretized into a mesh. Time is introduced in order to solve transient problems and is achieved through implementation of Newton's backwards difference method, which states,

$$\dot{U}_{t+\Delta t} = (U_{t+\Delta t} - U_t)(1/\Delta t) \tag{3.15}$$

Introducing this term into the energy balance (3.14) gives,

$$\frac{1}{\Delta t}\int_V N^N \rho\left(U_{t+\Delta t} - U_t\right)dV + \int_V \frac{\partial N^N}{\partial \mathbf{x}} \cdot \mathbf{k} \cdot \frac{\partial \theta}{\partial \mathbf{x}} dV - \int_V N^N r dV - \int_{Sq} N^N q dS = 0 \tag{3.16}$$

Solving a linear problem using FEA is done by solving the set of global equations for all elements as described by equations (3.5) and (3.16) for the complete structure; whereas solving a nonlinear or transient problem incorporates time into the model, where equation (3.5) is solved for each time increment. The time increment Δt is based on a user specified tolerance on the maximum temperature change allowed in a time increment.Abaqus utilizes a number of numerical methods, such as Newton's methods, to solve the above system of equations in order to achieve a converged solution (Abaqus Theory Manual, 2010).

## 3.3 Material Models and Model Assumptions

Steel and concrete work well together in reinforced concrete structures. High strength concrete is known to be an extremely brittlematerial (Marzouk 1992),which performs great under compression but has low failure strength when in tension. In order to mitigate this, steel-reinforced concrete was introduced. Steel was selected due to its high strength, high tensile strain, and the fact that it bonds well to concrete. The steel rods, or rebar, are incorporated into the concrete matrix to increase the strength of concrete in tension and bendingby transferring

tensile loads, resulting from pure tension or bending, to the steel while the concrete supports compressive loads (Askeland 2006).

As a first step to modeling a SRC column, a simple finite element model was constructed. For thisfinite element (FE) model, the representative volume element (RVE) in Figure 3.1 was used. Due to the symmetry available in standard RC columns, only a quarter section of the column will be analyzed to capture the full behavior of the column and attain accurate results. In order to further reduce the computational effort, it can be assumedthat for a long column completely exposed to the fire, the problem reduces to a 2D plane strain problem. This can be justified since the column will experience little to no out-of-plane deformation.

The contact between the concrete and the steel rebar are bonded together to prevent relative motion throughout the simulations. The bonding at the steel – concrete interface is achieved through utilizing "tie" constraintsbetween the nodes of the concrete and the nodes of the steel. These "tie" constraints couple the degrees of freedom of the nodes at the steel – concrete interface, which insures the two objects remain in contact (Abaqus Analysis User's Manual 2010). In order to prevent any artificial moments from forming at the coincident nodes due to a mismatch in node locations, the same number of nodes was used at the interface of both the steel and concrete. This guarantees that the nodes are unique yet coincident.

For the work in this chapter, the material models for concrete and steel were assumed to be linear and independent of temperature. It is well known that the properties of concrete and steel vary at high temperatures (Kodur et. al 2008,

Kodur et. al 2010), for instance both steel and concrete show significant softening at temperatures typically experienced in a fire. These changes have been neglected for this portion of the analysis for computational considerations. The model proposed in this chapter is used to establish an understanding of the failure mode of SRC columns under extreme fire conditions. These properties are summarized in Table 3.1.

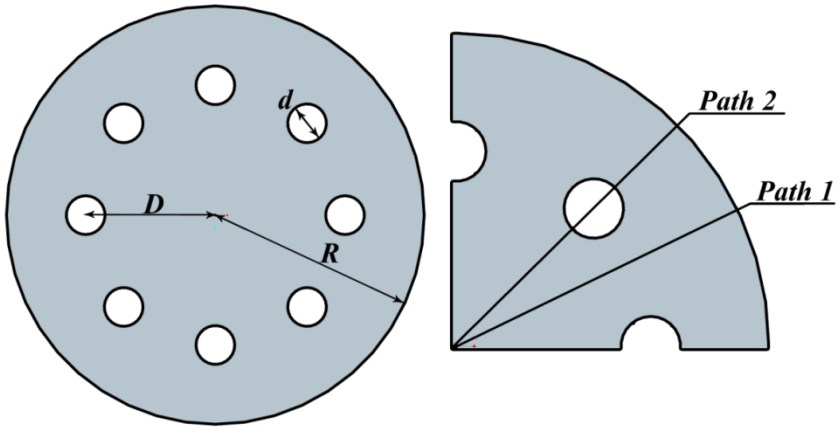


**Figure 3.1 (a) Cross Section of Strandard SRC Concrete Column and (b) FE Model RVE based on a Quarter of the SRC Column (not to scale)**

The next step in creating a FE model is the selection of an appropriate element type. The elements used for both the steel and concrete are 2D coupled temperature – displacement plane strain elements, CPE4T, which have 2 translational degrees of freedom in the x- and y- directions and 1 temperature degree of freedom at each of the four nodes (Abaqus Analysis User's Manual 2010). This element is bi-linear in both displacement and temperature, which implies that the shape function used to interpolate over the domain of the element is bi-linear in nature. This was selected over higher-order elements, such as the CPE8T element, which is quadratic in displacement and bi-linear in temperature,

due to the fact that a fine meshing scheme is being employed. The reasons and benefits of a fine mesh will be covered later in the section.

**Table 3.1**
**Material Properties of Concrete and Steel**

| Material Property | Concrete | Steel |
|---|---|---|
| **Density, ρ [kg/m$^3$]** | 2450 | 7850 |
| **Modulus of Elasticity, E [GPa]** | 20 | 200 |
| **Poisson's Ratio, ν** | 0.2 | 0.3 |
| **Coefficient of Thermal Expansion, α [/°C]** | $2.7 \cdot 10^{-6}$ | $5.3 \cdot 10^{-6}$ |
| **Emissivity, ε** | 0.9 | 0.9 |
| **Thermal Conductivity, k [W/(m·K)]** | 1.7 | 43 |
| **Specific Heat, $c_p$ [J/(kg·K)]** | 750 | 490 |

The properties of the concrete and steel represent a significant problem for meshing the RVE. The large differences in the moduli and thermal conductivity between the steel and concrete create an issue which arises from the tying of coincident nodes, as discussed previously, due to rapidly changing stresses. In order to mitigate this, the region surrounding the concrete/steel interface is finely meshed (*NAFEMS A Finite Element Primer* 1992). This fine mesh also allows utilizing linear elements, as opposed to more computationally expensive quadratic elements, without a significant loss in accuracy. Similarly, for the region of concrete between the rebar and the center of the column, the mesh becomes gradually coarser. The reason behind this meshing scheme is the temperature and strain distribution in the region around the steel rebar is what is of concern.

Thus,we can reduce the number of elements in this region since it is of no interest. The partitioning of the model and the result of the meshing scheme is shown in Figure 3.2. Additional information, regarding mesh convergence can be found in Appendix A.

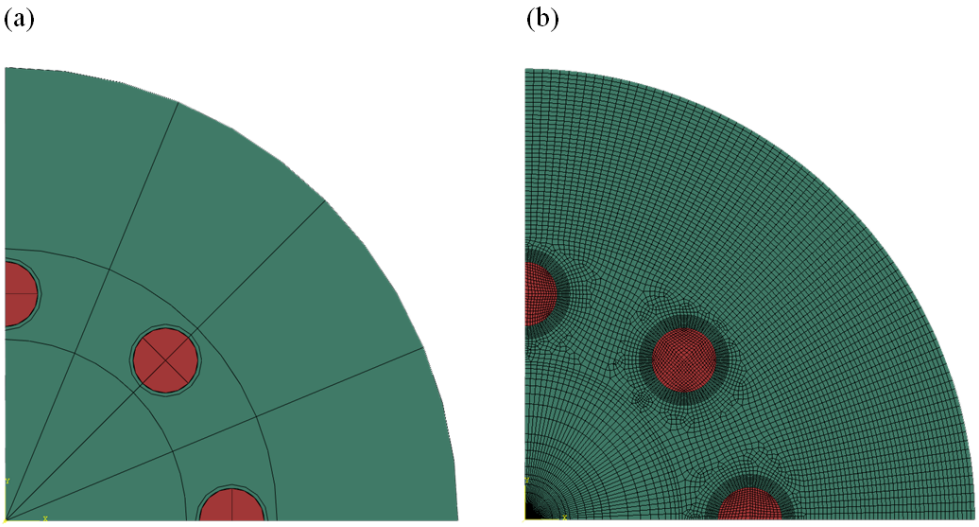


**Figure 3.2 A schematic showing (a) the partitioned model and (b) the applied meshing scheme**

Once the meshing was addressed, the next challenge was to decide on the appropriate boundary conditions and loads for the model. As discussed previously, the FE model will only take into account a quarter of the entire column's cross section. This assumption holds due to the symmetry the column has about both the x- and y- axis. In order to model this, an appropriate symmetry conditionwill be assigned in the FE model. Along the y-axis, the symmetry condition is realized in Abaqus using the *XSYMM command, which ensures that the degrees of freedom of the nodes associated with this edge are zero; U1 = UR2 = UR3 = 0. Similarly, along the x-axis, the symmetry condition is realized using the *YSYMM command; in this case U2 = UR1 = UR3 = 0 (Abaqus Analysis

User's Manual 2010). It is important to note that since 2D elements are used, all rotational degrees of freedom (UR1, UR2, and UR3) are not active degrees of freedom. Lastly, the thermal load is prescribed as a boundary condition on the outer surface of the column. For the simulations associated with this chapter, cases where the fire's temperature ranges from 500˚C to 1000˚C will be evaluated. The load line and boundary conditions are highlighted in Figure 3.3.

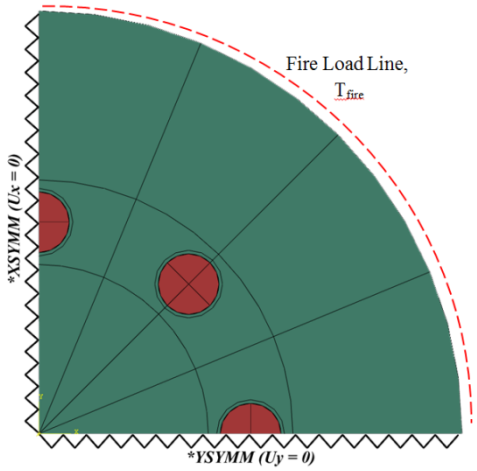


**Figure 3.3A schematic showing the boundary conditions and applied thermal load as applied in Abaqus.**

For the purpose of studying the effect of fire on reinforced concrete columns, several cases have been designed and simulated. These cases were designed to investigate both the effect of varying fire temperature on the failure of the column as well as the location of the steel rebar within the column. These cases and the associated failure times are summarized in Table 3.1.

**Table 3.2**
**Summary of Cases for Characterising SRC Coulm Failure**

| Case No. | Beam Geometry [m] | As/At (%) | Fire Temperature [C] | Failure Time [min] |
|---|---|---|---|---|
| **1** | R = 0.2;<br>d = 0.02865<br>D = 0.1 | 4.1 | 700 | 191 |
| **2** | *Same as Case 1* | | 800 | 170 |
| **3** | *Same as Case 1* | | 900 | 153 |
| **4** | *Same as Case 1* | | 1000 | 140 |
| **5** | R = 0.2<br>d = 0.02865<br>D = 0.05 | 2.85 | 1000 | 165 |
| **6** | Same as Case 5 but D = 0.1 | *Same as Case 5* | | 159 |
| **7** | Same as Case 5 but D = 0.15 | *Same as Case 5* | | 152 |

3.4 Fire Failure Mode of a Reinforced Column

The main objective of the cases listed in Table 3.2 was to gain an insight into the mode of failure of a SRC column in a fire situation, and how different configurations of the rebar affect the overall fire resistance of the column. It is hypothesized that as the column heats up, the difference in CTE between the steel and concrete will create a stress concentration in the region around and between the steel rebar. Thus, one major factor in determining the fire resistance in the column is, naturally, the temperature of the fire and the rate at which the column heats up.

Figure 3.4 illustrates the temperature of the steel – concrete interface over the duration of the simulation for Cases #1 – 4. It is observed that the temperature of the fire has a large impact on the rate at which the column heats up. Another factor which should be taken into consideration, but not modeled in the simulations as it is outside the scope of this research, is spalling.Spalling, which is

the removal of concrete from the surface of the column, becomes critical since it is more prevalent in high strength concrete than normal concrete ; this is due to its reduced porosity and because it is more likely to occur under rapid heating, such as that experienced in a fire. Spalling is dangerous in SRC columns because, as more concrete is removed from the surface of the column, the rebar can become directly exposed to the fire which results in a rapid decrease of the load bearing capacity of the column (Anderberg 1997, Hernández-Olivares 2003).

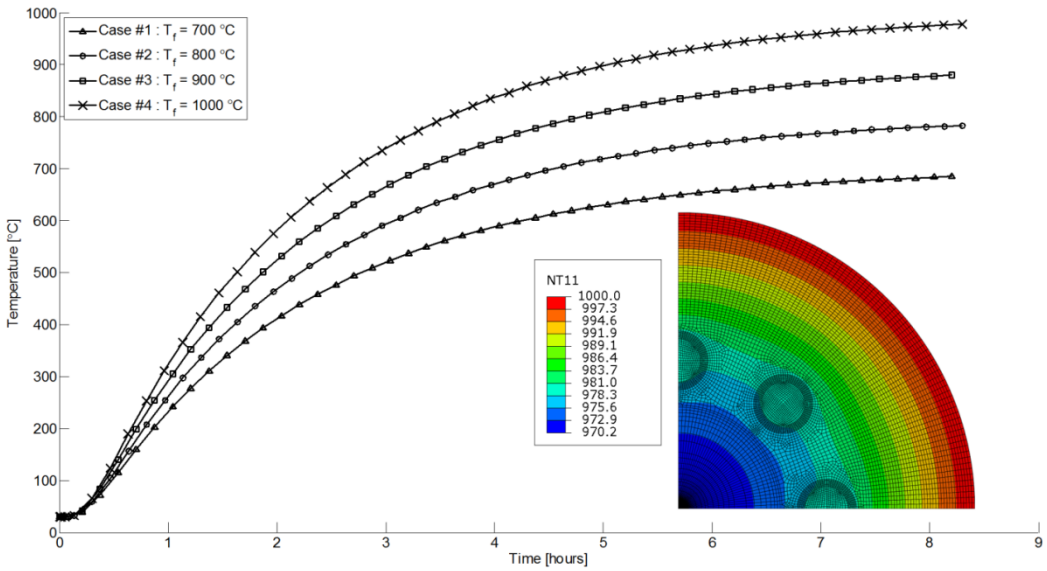


**Figure 3.4 Temperature of Steel Rebar for Cases #1 – 4 over the Duration of the Simulation**

While the temperature of the column is of importance, it is ultimately the strain that dictates failure. It is clear from Figure 3.5that the largest values of strain in the column are at the steel – concrete interface. All measurements of strain and temperature in this study are taken at the steel – concrete interface because once the concrete begins to fail at the interface,delamination of the steel and concrete occurs, which leads to cracking of the concrete. These cracks grow and join together creating a fracture plane (Li 2007). The delamination of the steel

weakens the overall column and the fracture planes within the concrete further accelerate the weakening and failure of the concrete. This goes in line with the original hypothesis that the failure would be based on the expansion of the steel rebar within the column.

For the purposes of this chapter, a simple failure criterion was used, which states that failure of the column occurs once the strain at the interface exceeds the failure strain of $\varepsilon_f = 0.4\%$ (Nataraja 1999). Thus the strains were plotted versus time, and the time taken for the simulated strain to exceed the failure strain was considered the column's fire resistance. These times were listed in Table 3.2. It is clear that as the temperature of the fire increases, the fire resistance of the column decreases and as such two conclusions can be made: (1) the fire resistance is inversely proportional to the temperature of the fire and (2) the primary mode of failure in the column is due to the rapid expansion of the steel rebar against the concrete due to the mismatch in CTE. This expansion results in large strains at the steel – concrete interface resulting in delamination, which significantly reduces the load bearing capability of the column.

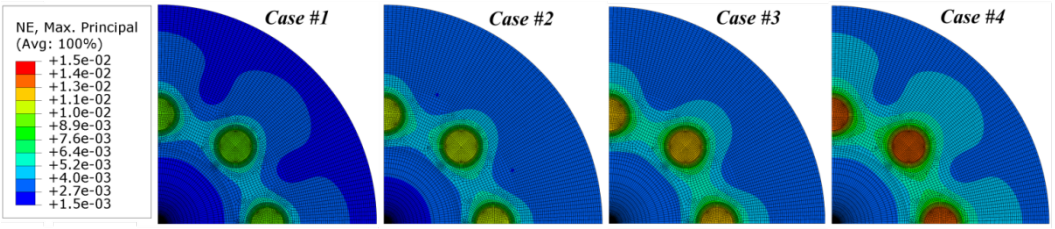


**Figure 3.5 A series of contour plots illustrating strain distribution for Cases #1-4 after 8 hours**

Closer examination of Figure 3.5 shows that the strain along a path from the center of the column to the edge, and which does not pass through a

rebar(designated Path 1 in Figure 3.1), experiences significantly less strain than a path taken from the center of the column to the edge, and which does pass through the rebar (designated Path 2 in Figure 3.1).The reason for such a difference is because the effect of the rebar's expansion reduces asyou move away from the rebar and as such the strain decreases.This would indicate that the radius of the rebar array might play a role in determining the fire resistance of the column; as the rebar radius decreases, the distance between two subsequent rebar decreases. In order to investigate this relationship, Cases #5 – 8 were designed and simulated.

At first inspection, and in light of the previous statement, it would be considered ideal to move the rebar away from surface of the column to reduce the temperature of the rebar. The lower the temperature of the rebar, the slower the rebar will expand and should thus ultimately lead to an improvement of the column's fire resistance. This assumption though is flawed as it does not take into consideration the fact that as the rebar is moved closer to the center, i.e. the rebar array radius is reduced, the distance between one rebar and the next is also reduced. This effect can be seen in Figure 3.7. As the rebar move closer together, the concrete between two neighboring columns will experience the compressive forces of both expanding rebars which will accelerate the failure of the concrete. It can be observed in Figure 3.6 that for Case #5, the strain in the concrete between the rebar, Path 1, is of the same order as that of the strain in the steel. In comparison, Case #7 shows a distinct difference between the strain levels of Path 1 and 2.

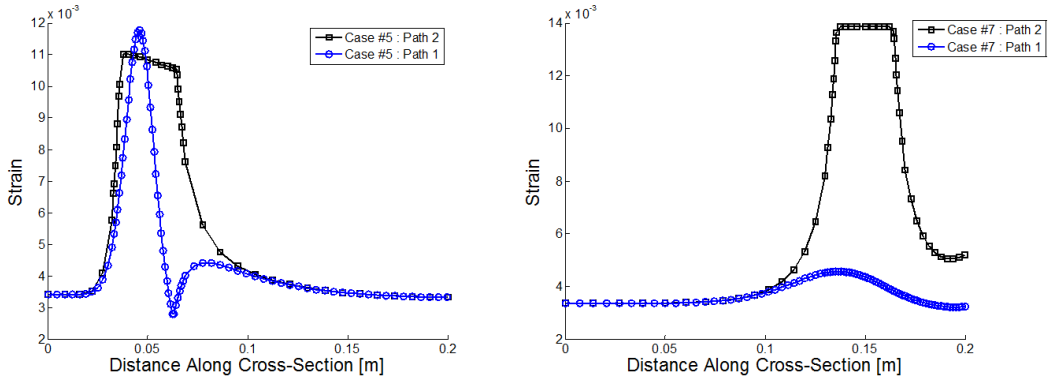


**Figure 3.6 Plot of the Max Principal Strain Along Path 1 and 2 for Case #5 and Case #7 after 4 hrs.**

These results are significant because in the event of failure in Case #5, the results are even more catastrophic due to the fact that all the concrete around the rebar and in between the rebar will fail at nearly the same time. This could lead to a region of failure that bisects the column and essentially creates an inner column (the region between the rebar and the center of the column) and an outer hollow cylindrical column (the region from the rebar to the surface of the column). This could drastically reduce the load bearing capability of the column.

For Case #7, as the rebar moves closer to the surface of the column, they experience a quicker rise in temperature due to the close proximity to the fire. This will result in a more rapid expansion of the steel rebar and subsequent compression of the concrete which ultimately leads to a quicker failure of the column. It could be observed from both Figure 3.6 and Figure 3.7 that the strain levels in the concrete between the rebar is significantly less than in the immediate vicinity of the rebar. Failure of the concrete at the steel – concrete interface results in delamination of the concrete from the steel and in the absence of this bond, the

concrete can no longer transfer load to the steel which reduces the load carrying capability of the column.The failure times for Cases #5-7, as well as the previous cases, can be found in Table 3.2.

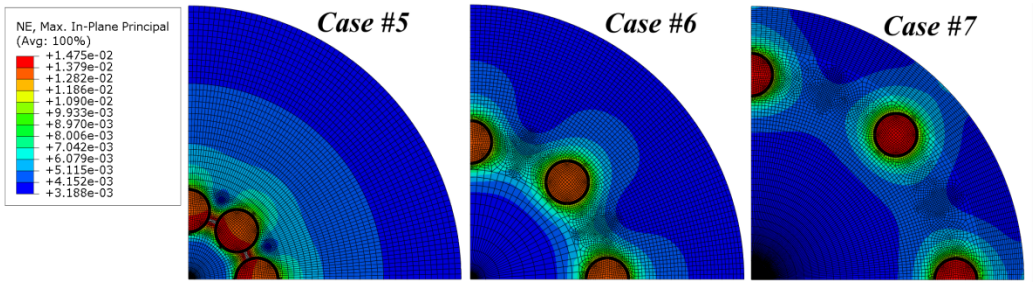


**Figure 3.7 A series of contour plots illustrating strain distributions for Cases #5 - 7 after 8 hrs.**

To further investigate the location of initial failure, a simple simulation was designed to look at failure at the column/floor joint. Typically, a column is fixed at both ends and thus the boundary conditions would imply that no deformation can occur at these joints. In previous simulations, the outside edge of the column was allowed to freely expand. This was done to model any section of the column away from the joints. Previous results indicate that the maximum levels of strain were at the steel – concrete interface. In order to show that the confinement of the concrete at the outer edge did not change this result, the following simulation was performed. The outer edge of the column was confined using the encastre command, which ensures that the degrees of freedom of the nodes associated with this edge are zero; U1 = U2 = U3 = UR1 = UR2 = UR3 = 0. All other parameters remained constant to those described in Table 3.4 (Case #4).

As is illustrated in Figure 3.8(a), the confined edge causes the level of strain near the edge to increase over the column with a free expanding edge

(Figure 3.8(b)). This is to be expected because the increase in temperature will cause an expansion in the concrete, and if it is not allowed to expand, it will compress into itself, thus generating high levels of strain. While this is the case, it is also evident that the highest levels of strain are still associated with the steel – concrete interface.This can be explained by the fact that the steel continues to expand at a quicker rate then that of the concrete. As such, it remains the major factor in the failure of the column

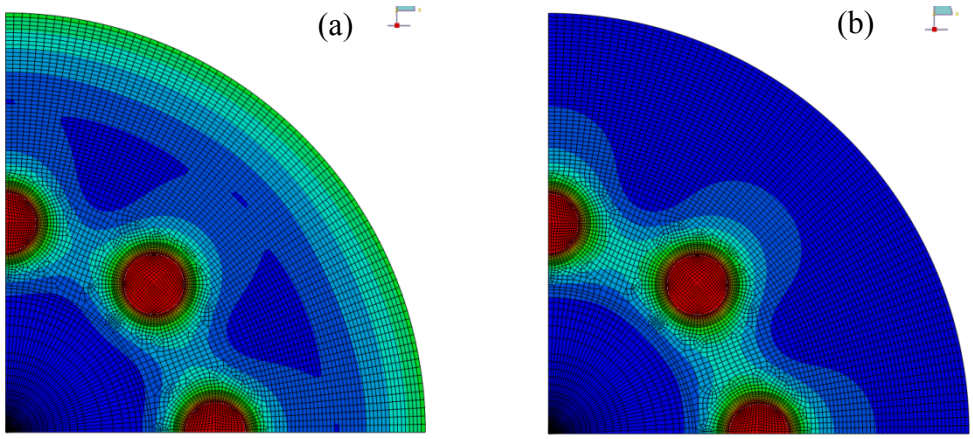


**Figure 3.8 A series of contour plots illustrating difference in strain levels between (a) column confined from expanding at outer edge and (b) column free to expand at outer edge**

## 3.5 Summary

Several cases have been simulated in order to determine the mode of failure of a steel reinforced concrete column in a fire situation. It has been found that the mismatch in the coefficient of thermal expansion between the concrete and the steel results in steel expanding quicker than the surrounding concrete, which creates a region of high strain in the concrete. The levels of strain quickly reach failure levels before any other location in the column. Further testing was done to establish the relationship between the location of the rebar and the failure

time of the column. This understanding allowedapproaching the concept of improving the fire resistance of a column by addressing the main factor, which is heat propagation within the column.

# Chapter 4

# EFFECTS OF CRUMB RUBBER CONCRETE ON FIRE RESISTANCE OF SRC COLUMNS

## 4.1 Introduction

The analysis in Chapter 3 considered the effects of fire on a steel reinforced concrete column, and the primary mode of failure due to the heating of the columnwas alsoinvestigated. Numerous cases were simulated, and it was determined that the expansion of the steel rebar caused by the mismatch in CTE was the primary cause for failure. These results, however, were based on models that incorporated material properties which remained constant with temperature. Furthermore, the applied thermal load was at constant temperature; whereas, for realistic modeling and testing, the fire model should follow that of the ASTM E119-00 standard. To getmore accurate results, the following chapter will incorporate models for high strength concrete (HSC) and structural steel based on models derived from the ACI and others (“*ACI Manual of Concrete Practice” 2000, Kodur 2004)*.

With the emergence of high strength concrete and high strength steel, it has become evident that the fire performance of HSC differs from those of normal strength concrete (NSC) and does not perform well in fires (Kodur 2004). This inherent behavior of HSC in high temperature fires, along with the expansion of HS steel could greatly reduce the fire resistance of a load bearing columns. Because of this, it became of interest to introduce and implement an insulating

layer structure. In this research study, crumb rubber concrete (CRC) was used for this purpose.

Crumb rubber is a material produced by shredding used tires. Various studies looked into the use of crumb rubber in concrete as a wayto improve the performance of PCC in numerous situations (Shimizze 1994, Biel 1994, Toutanji 1996, Fedroff 1997). These studies exploited the crumb rubber additives as simple concrete fillers to enhance the performance of concrete in thermal expansion/contraction and freezing conditions.

In this research work, the effect of a 2cm thick CRC region integrated within the reinforced concrete (RC) column was investigated. The simulation explores the effect that a region of CRC, with a fixed volume fraction, has on the fire resistance of a column. By varying the position of the CRC region, the effects on strain and temperature can be determined. Furthermore, by evaluating the failure strain for each case, an approximation for the fire resistance of the column can be calculated.

## 4.2 Analysis Procedure

For this investigation, the meshing technique and element type (plane strain) discussed earlier was again used. The analysis setup regarding the thermal load line as well as the symmetry conditions was also similar to what was presented earlier in Chapter 3. The difference from the previous analysis was the inclusion of a region of crumb rubber concrete incorporated within the standard SRC column as shown in Figure 4.1. By introducing this CRC region with a thickness equal to 10% of the column's radius, it would act as a thermal barrier

within the column in anticipation of abating the heat propagation within the column by exploiting the thermal properties of the crumb rubber. The inclusion of rubber particles within the concrete matrix will act as a thermal barrier as well as an absorber of the thermal energy; thus, reducing the amount of energy in the concrete which will lead to a reduction in the rate at which the temperature propagates within the column.

Further improvements included the introduction of accurate material models for HS concrete and high strength structural steel. These material models are critical for obtaining accurate results since they take into account the dependencies of various material properties on temperature. These properties include the elasticity, specific heat capacity and thermal conductivity. Both materials have models for thermal strain which are linear with temperature, thus implying a constant value for the CTE (Youssef 2007). Further discussion on the material properties will be covered in a later section.

In addition, for the models described in this chapter, it is assumed that the surface of the column is prescribed with a temperature boundary condition which follows that of the standard fire exposure described in ASTM E119-00 (*ASTM Standard Test Methods for Fire Test of Building Construction and Materials*, 2000). The temperature can be approximated by the following expression (Kodur 2003):

$$T_f = T_o + 750\left[1 - \exp\left(-3.79553\sqrt{\tau}\right)\right] + 170.41\sqrt{\tau} \quad (4.1)$$

*where* :

$\tau$ = time (hours)

$T_0$ = initial temperature (°C)

$T_f$ = fire temperature (°C)

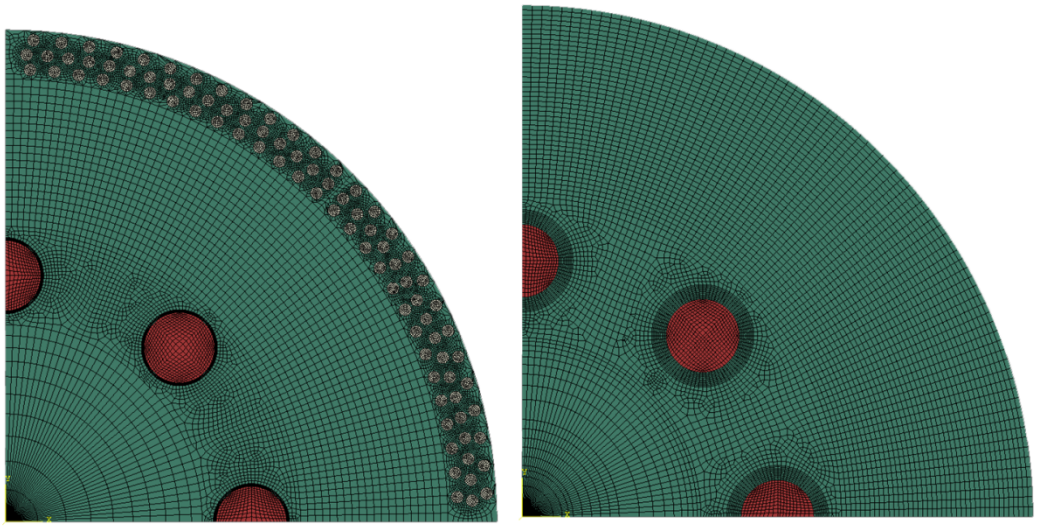

**Figure 4.1 Finite Element Model of SRC Column with and without CRC region after meshing**

In order to achieve a reasonable understanding on the effect of the CRC region incorporated into a SRC column, five different cases are investigated, in which the radius of the CRC region is varied from 0.125 to 0.19 m. This will facilitate the determination of what effect the location of the CRC region will have on the fire resistance of the SRC column.

It is predicted that for the case of the CRC region closest to the surface, R = 0.19m, will perform the best due to the blunting of temperature propagation right at the surface, thus reducing the core temperature more effectively.

## 4.3 Material Models

The effects of temperature on the constitutive relations of the column's materials are of great importance when generating an accurate FE model. These properties include, but are not limited to, thermal conductivity, specific heat capacity and thermal coefficient of expansion. For this model, the relationships for these parameters will be used in accordance with the results derived from experimental results (Kodur 2008, Eurocode EN1992-1-2, ASCE Structural Fire Protection Manual 1992, Youssef 2007). In the simulation, the use of high-strength concrete with a carbonate-type aggregate is assumed.The models state that:

$$c_c = \begin{cases} 900, & \text{for } 20°C \le T \le 100°C \\ 900 + (T - 100), & \text{for } 100°C \le T \le 200°C \\ 900 + -0.5 \times T, & \text{for } 200°C < T \le 400°C \\ 1100, & \text{for } 400°C < T \le 1200°C \end{cases} \tag{4.2}$$

$$k_c = \begin{cases} 0.85 \times (2.0 - 0.0013 \times T), & \text{for } 20°C \le T \le 300°C \\ 0.85 \times (2.21 - 0.002 \times T), & \text{for } 300°C < T \end{cases} \tag{4.3}$$

$$\frac{E_{c,T}}{E_c} = \begin{cases} 1.0 - 0.0015 \times T, & \text{for } 20°C \le T \le 200°C \\ 0.87 - 0.00084 \times T & \text{for } 200°C \le T \le 700°C \\ 0.28 & \text{for } 700°C \le T \end{cases}$$

*where*,

$c_c$ = Specific heat of concrete at at temperature T

$k_c$ = Thermal conductivity of concrete at temperature T

$E_c$ = Modulus of Elasticity of concrete at 20°C

$E_{c,T}$ = Modulus of Elasticity of concrete at temperature T

(4.4)

It is worth mentioning that equation (4.4) stipulates that concrete is a linear elastic material. In reality it has been very well documented that concrete

exhibits a non-linear hypereleastic relation (Balan 2000, Kodur 2008, Youssef 2007) and whose constitutive model is described by,

$$\sigma_c = \begin{cases} f'_{c,T}\left[1 - \left(\dfrac{\varepsilon - \varepsilon_{\max,T}}{\varepsilon_{\max,T}}\right)^2\right] & , \varepsilon \le \varepsilon_{\max,T} \\ f'_{c,T}\left[1 - \left(\dfrac{\varepsilon_{\max,T} - \varepsilon}{3 \cdot \varepsilon_{\max,T}}\right)^2\right] & \varepsilon > \varepsilon_{\max,T} \end{cases} \tag{4.5}$$

where $\sigma_c$ is the compressive stress in the concrete and $\varepsilon$ is the instantaneous strain in the column. $f'_c$ is the compressive strength, which is a function of temperature and is described in equation (4.6). $\varepsilon_{max,T}$ is the concrete strain at maximum stress for a given temperature T and is described in equation (4.7).

$$f'_{c,T} = \begin{cases} f'_c & ,20°C \le T \le 450°C \\ f'_c\left[2.011 - 2.353\left(\dfrac{T-20}{1000}\right)\right] & ,450°C < T \le 874°C \\ 0 & 874°C < T \end{cases} \tag{4.6}$$

$$\varepsilon_{\max,T} = 0.025 + \left(6.0T + 0.04T^2\right) \times 10^{-6} \tag{4.7}$$

Although Abaqus is capable of handling such non-linear material models, the simulations in this chapter utilized the linear elastic model in order to reduce the computational time.It was also noticed that there was no difference observed in the temperature or strain values when comparing the linear elastic model to the hyperelastic model. As discussed in section 3.2, Abaqus calculates the displacement of each element, from which the strains and then stresses are

derived. As such, only the values of stress will be altered by using a linear elastic model. This is satisfactory for this work since all failure criterions are based on strain in the concrete and not the stress.

For the steel rebar, the model assumed that the steel is structural steel as defined by the ASCE standards. The models for the thermal and mechanical properties, as a function of temperature, were based on the ASCE models as put forth by (Kodur 2010). The model states that:

$$\rho_s c_s = \begin{cases} (0.004T + 3.3)\times 10^6, & \text{for } 20°\text{C} \le \text{T} \le 650°\text{C} \\ (0.068T - 38.3)\times 10^6, & \text{for } 650°\text{C} \le \text{T} \le 725°\text{C} \\ (-0.086T + 73.35)\times 10^6, & \text{for } 725°\text{C} < \text{T} \le 800°\text{C} \\ 4.55\times 10^6, & \text{for } 800°\text{C} < \text{T} \end{cases} \tag{4.8}$$

$$k_s = \begin{cases} -0.022T + 48, & \text{for } 20°\text{C} \le \text{T} \le 900°\text{C} \\ 28.2, & \text{for } 900°\text{C} < \text{T} \end{cases} \tag{4.9}$$

$$\frac{E_{s,T}}{E_s} = \begin{cases} 1.0 + \dfrac{T}{2{,}000 \ln\left(\dfrac{T}{1{,}100}\right)}, & \text{for } 20°\text{C} \le \text{T} \le 600°\text{C} \\ \dfrac{690 - 0.69T}{T - 53.5} & \text{for } 600°\text{C} \le \text{T} \end{cases}$$

*where*, (4.10)

$c_s$ = Specific heat of steel at at temperature T

$k_s$ = Thermal conductivity of steel at temperature T

$E_s$ = Modulus of Elasticity of steel at 20°C

$E_{s,T}$ = Modulus of Elasticity of steel at temperature T

A similar discussion can be made for the steel. It is well known that steel exhibits a very pronounced transition to the plastic region. However, the strains experienced by the steel in these simulations are rather small and as such the steel remains in the elastic region. For this reason, only the effect of temperature on the elasticity was modeled, as seen in equation (4.10) and not the plasticity.

Crumb rubber is generated from the shredding of used or defective automotive tires. They are comprised of a mixture of vulcanized styrene-butadiene-rubber (SBR), natural rubber, steel tread, carbon black fillers, and numerous other additives (Belyayeva and Fel'dshtein 1973; Kim *et al.*, 2000; Mastral *et al.*, 2002, Fernandez-Derridi, 2006). Due to the lack of data characterizing the properties of SBR or crumb rubber at high temperatures, it was assumed that all properties, thermal and mechanical, remained constant up to the degradation temperature, $T_d$, at which point they are reduced to zero, as shown in equations (4.11) – (4-13). For this simulation, it was assumed that the degradation temperature was 450˚C based on the findings of Halasa (2005). A more in depth look of the various material models for concrete, as well as illustrations of the aforementioned models are given in Appendix B.

$$\frac{c_{R,T}}{c_R} = \begin{cases} 1, & \text{for } 20°\text{C} \le \text{T} \le \text{T}_\text{d} \\ \sim 0, & \text{for } T_\text{d} \le \text{T} \end{cases} \tag{4.11}$$

$$\frac{k_{R,T}}{k_R} = \begin{cases} 1, & \text{for } 20°\text{C} \le \text{T} \le \text{T}_\text{d} \\ \sim 0, & \text{for } T_\text{d} \le \text{T} \end{cases} \tag{4.12}$$

$$\frac{E_{R,T}}{E_R} = \begin{cases} 1, & \text{for } 20°C \le T \le T_d \\ \sim 0, & \text{for } T_d \le T \end{cases}$$

*where*,

$c_{R,T}$ = Specific heat of steel at at temperature T (4.13)

$k_{R,T}$ = Thermal conductivity of steel at temperature T

$E_R$ = Modulus of Elasticity of steel at 20°C

$E_{R,T}$ = Modulus of Elasticity of steel at temperature T

## 4.4 The Effects of an Insulating Crumb Rubber Concrete Region

The primary objective of this chapter is to quantify the improvement, if any, of a CRC region has on the fire resistance of a SRC column. In order to establish this, the values of the maximum principle normal strain were extracted for each case. A failure theory based on the normal stress/strain (Rankine's Theory) was selected since concrete exhibits brittle behavior for which a max normal stress/strain theory is most accurate (Collins 1993).

It was determined that failure would be calculated in the concrete surrounding the steel rebar since it will be under compression, as opposed to the outer region of the column which will experience free expansion. Furthermore, as discussed in Chapter 3, delamination at this interface is a primary cause for weakening and failure of a concrete column. As a failure criterion, the column was assumed to fail when the strain in the region surrounding the rebar exceeded the maximum strain for concrete as derived by Li and Purkiss (2004). As can be seen in equation (4.14), the value of maximum strain is highly dependent on the temperature of the concrete. Since the inclusion of crumb rubber concrete will

result in a temperature gradient that will vary from case to case, failure strain must be evaluated for each case independently. It is important to note that all measurements of temperature and strain were taken at the steel-concrete interface due to reasons previously discussed.

$$\varepsilon_{\max} = \frac{2 \times f'_c}{E_{ci}} + 0.21 \times 10^{-4}(T - 20) - 0.9 \times 10^{-8}(T - 20)^2$$

*where*,

$\varepsilon_{\max} =$ Strain at max value of stress (4.14)

$f_c^{'} =$ Compressive strength of concrete

$T =$ Temperature during simulation

For purpose of studying the effect of a CRC region, numerous cases were constructed and simulated. The purpose of these different cases was to investigate the effect that positioning of a CRC region has on the fire resistance of a column. The volume fraction and rubber particle size were fixed for each case at 40% and 5mm respectively.The radius of the band was varied from 0.125m to 0.19m. The column's radius was also fixed at 0.20m.

Figure 4.2 shows the final results of the temperature tests for the control and all cases. Visual inspection shows that the 3rd heat band from the outside, which corresponds to a temperature of 1000˚C, never fully propagated to the steel in any of the cases as it did in the control. This clearly shows that adding a layer of crumb rubber to the SRC slows the heat propagation in the column.

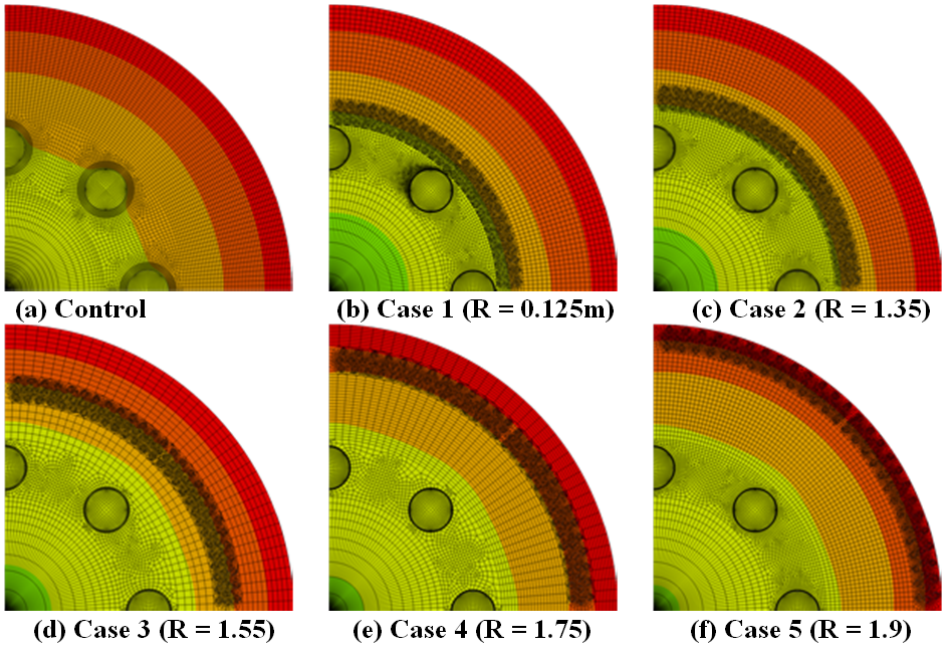


**Figure 4.2 A series of contour plots illustrating temperature propagation after ~16.5 hours for control and Cases 1-5**

Figure 4.3 plots three of the five cases against the control to further illustrate the reduction in temperature. It shows a mostly constant decrease in core temperature throughout the entire simulation. It was hypothesized that the best results for a reduction in temperature propagation would be for Case 5 because the rubber inclusions were on the outermost layer. However, the results show that Case 1 actually slowed the heat propagation the most with a difference of about 60˚C at the end of the experiment. As the rubber region was moved away from the center in Cases 2 – 5, the final temperature difference decreased to about 45˚C. This can be attributed to the fact that as the CRC region moves towards the outer edge, there is less concrete between the rubber and the heat source. This extra concrete acts as an insulator between the heat source and the rubber, which slows the heat propagation to the rubber and delays the degradation of the rubber

inclusions. Because the rubber closest to the core will heat up slower, it will reach its degradation temperature at a later time and will act as the main insulator for a longer duration. As a result, the strain in the core will also be reduced.

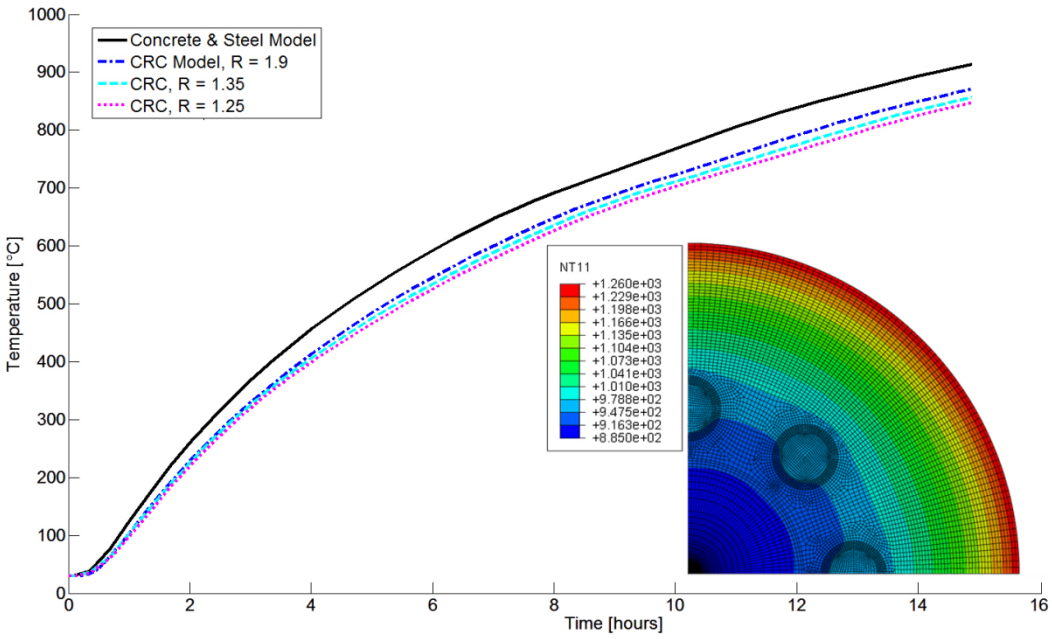


**Figure 4.3 Temperature of the steel – concrete interface over the course of the simulation for the Control Case and Cases #1,2 and 5**

Furthermore, it can be seen that the inclusion of the crumb rubber has significantly reduced the rate at which the column is heated which would have a profound effect on preventing spalling. In addition to the reduction in rate of heating, the rubber inclusions themselves act to improve the porosity of the HS concrete thus creating pockets for the water vapor to escape through (Kodur 1998). Also, it has been found that spalling typically occurs at the surface of the column (Hernandez-Olivares 2003). For Case #5, where the CRC region is located at the surface, it could further reduce the possibility of spalling and if

spalling were to occur, the rubber could potentially dampen the explosive effects of spalling.

In order to determine the effect of the CRC region on the strains generated within the column, contour plots of the maximum principle strain for each case were created (Figure 4.4). Comparing Figure 4.4(a) to Figure 4.4(f), it is clear that the strain concentration in the concrete region between the steel rebar is lessened with the rubber inclusions. This is true for all the cases, but the difference is greatest, as previously stated, for Case 1. In order to fully understand the effects of this, the strain at the steel-concrete interface was plotted against time in Figure 4.5 for the control and Case 1 using the ABAQUS data and the curve derived from equation (4.14).

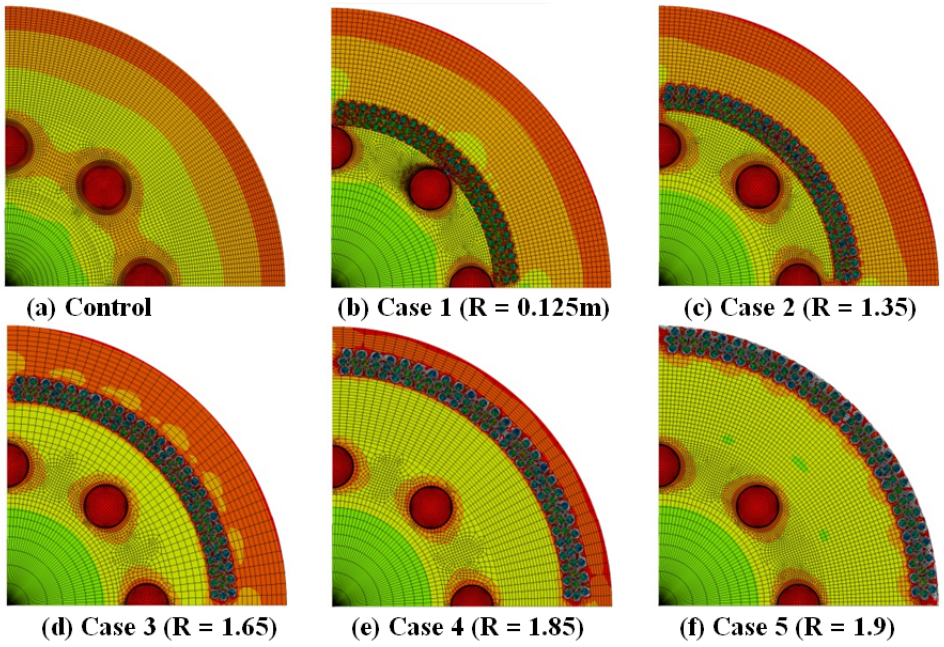


**Figure 4.4 A series of contour plots illustrating strain distribution after ~16.5 hours for control and Cases 1-5**

Failure time is calculated from Figure 4.5 by determining the crossover point between the curve generated by equation (4.14) and the ABAQUS data. For the control, failure time occurs at approximately 3.5 hours. Adding a concrete-rubber layer at a radius of 0.125m delays the failure time by approximately 45 minutes. This is a significant increase in failure time, approximately 20%. Similar plots were created for each case, and the resulting associated improvement in failure times are plotted in Figure 4.6.

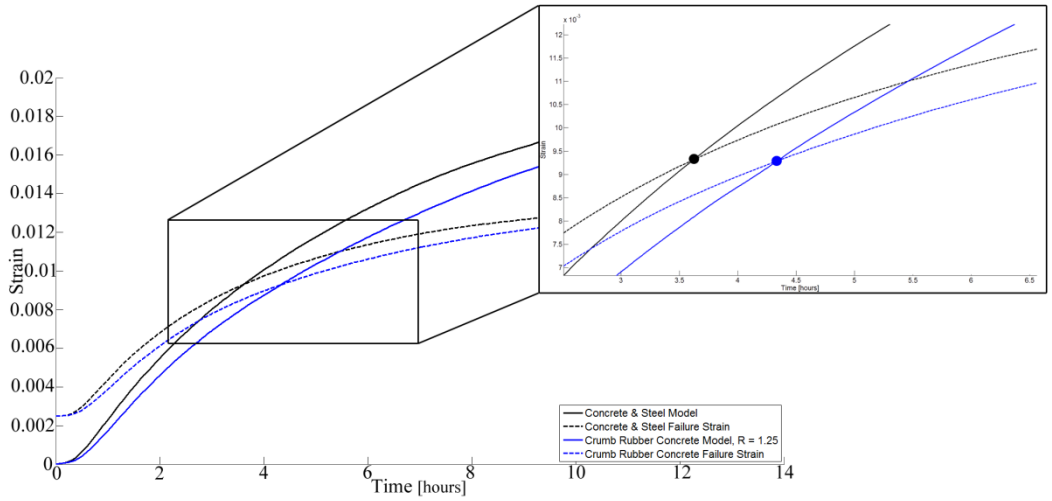


**Figure 4.5 Strain of concrete at steel – concrete interface over the course of the simulation and determination of failure time (inset)**

Although the improvement in failure time for Case 1 is the highest, Case 5 shows an improvement in failure time of approximately 34 minutes, which is still a significant value. Taking into consideration the manufacturing of a column with rubber inclusions, Case 5 offers the easiest approach because only one extra step is needed in the manufacturing process; it could easily be added to existing concrete columns. The small difference in time added between Case 1 and Case 5 is not significant enough to warrant an extra step in manufacturing and potential reduction in the column's strength. Therefore, the best case for application is arguably Case 5.

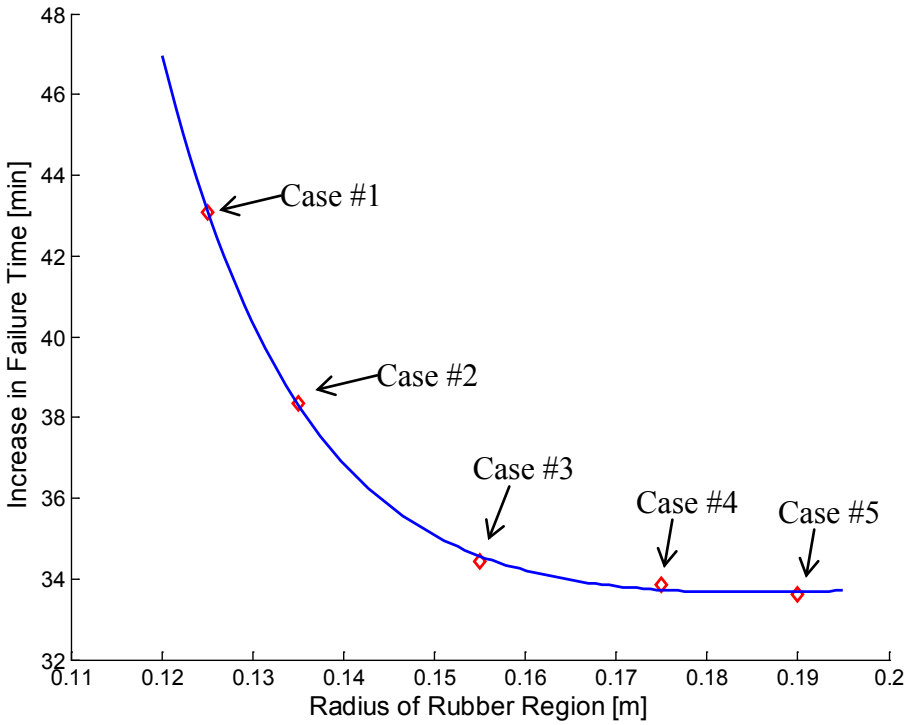


**Figure 4.6 Plot illustrating the increase in failure time for each case study of varying radius of the CRC region**

### 4.4.1 Effects of CRC on Resonant Frequency of Column

When modifying a critical, load bearing column, it is important to ensure that the structural integrity of the column is not hampered in any way. In many regions of the world, earthquakes pose a large danger to building. As such, a small study was conducted to analyze the effect that placing a crumb rubber concrete region would have on the natural frequency of the column. The inclusion of a CRC region results in an overall system that has a reduced mass and stiffness, mainly due to the fact that the stiffness of rubber is several orders of magnitudes less than that of steel, and since the natural frequency, $\omega_n$, is a function of both stiffness and mass, it is important to ensure the resonant frequency of the column is not severely reduced.

In order to test this, two cases were simulated; the control case and Case #5. Their natural frequencies were calculated using Abaqus. Figure 4.7 shows the first four resonant frequencies for both cases. It can be seen that in fact the resonant frequencies for Case #5 are indeed lower that the control case. The difference varies from 1.1% for the first mode shape (natural frequency) to 11.2% for the fourth mode shape. Since the first mode shape is typically the most predominate, a difference of 1.1% is negligible and thus we can conclude that the addition of a CRC region to the outside edge of the column has little to no effect on the natural frequency of the column. In fact, the addition of rubber may actually enhance the damping capability of the column.

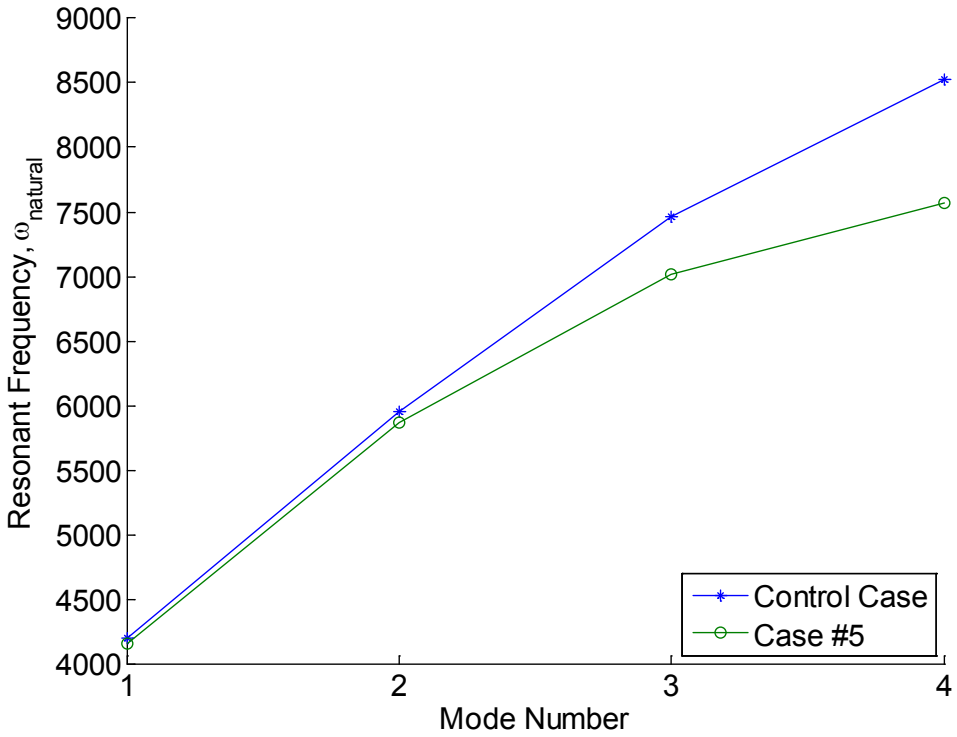


**Figure 4.7 Comparison of first 4 resonant frequencies between the Control Case and Case #5**

## 4.5 Summary

Steel reinforced concrete columns are common in buildings all over the world. Recent advances in high strength SRC has led to columns that are more susceptible to failure due to fire. Therefore, it will be necessary to provide a means of protecting the column from fire conditions in order to increase the failure time of the column. In this study, a crumb rubber concrete layer was introduced to protect the SRC during fire conditions;five cases with various positions of the CRC layer were simulated in Abaqus. It was found that by adding a CRClayer to the column at any radius shows a significant delay the column's failure time. The best reduction time is realized by adding the rubber region closest to the steel. However, due to constructability and structural design

considerations, the best case was determined to be where the CRC layer is added at the outermost region (Case 5). Case 5 showed a significant improvement of 32 minutes in column failure time, and because the rubber is added on the outermost layer, this method of insulation could be added to any existing SRC columns.

# Chapter 5

# EFFECT OF CRUMB RUBBER VOLUME FRACTION ON COLUMN PERFORMANCE

## 5.1 Introduction

The analysis thus far has focused on the effect of the position of the CRC region within the column and preliminary results have shown a significant improvement in the fire resistance of the column. However, these results come from a model which maintains a significantly high volume fraction of rubber (40%) within a fixed thickness of 2 cm in a column with a radius of 20cm. While this small layer has shown significant improvements, it does not take into account a number of parameters including the effect of volume fraction on the strength of the column and the aggregate size used in the column. This becomes an issue because if the insulating layer is to be used in conjunction with the existing column as a load-bearing element then care must be taken to insure that the strength of the column is not compromised. In addition, concrete mixtures incorporate some form of fine aggregate into the mix to alter the properties of the concrete (Askeland 2006). This plays a big role in the design of the CRC region since the size and amount of fine aggregate plays a role in the amount (volume) of rubber that could be incorporated. The ACI Standard 211.1-91states that the average aggregate size for Portland cement concrete (PCC) varies from 1cm to 10cm (ACI Manual of Concrete Practice 2000).

The effect that the crumb rubber volume fraction has on the properties of concrete has been effectively studied by Kaloush (2006) and Lingannagari (2007). It was shown that as the volume fraction of rubber is increased the compressive strength significantly decreased although the peak axial strain was 6 – 10 times higher for larger crumb rubber volume fractions (Kaloush 2006). The study also showed that as CR content increased, the CTE of the overall mixture decreased. It is important to note that, as discussed earlier, the main cause of failure was the mismatch in CTE between the concrete and the steel. Thus it is recommended that the CRC not be paired or bonded to steel rebar as the larger mismatch in CTE would cause failure strains to occur sooner.

Thus the goal of the following analysis is only to investigate what effect the volume fraction of CRC has on the failure time of the column. This test simulates the addition of largeaggregates into the concrete mixture as the inclusion of aggregates ultimately determines the amount and distribution of the CR. The models tested in this section are designed to investigate a uniform reduction in volume fraction from 40% (Case #4) down to 10% (Case #1) and ultimately compared to the control case which contains no crumb rubber layer (Figure 5.1).

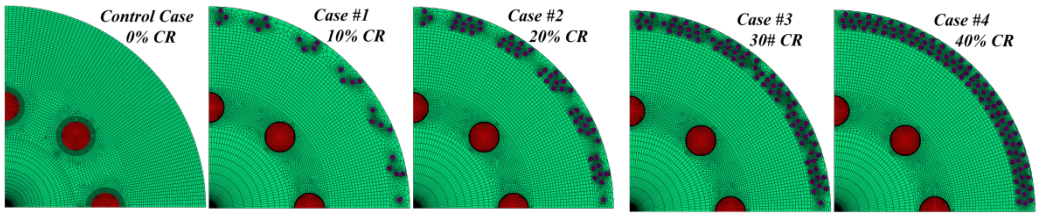


**Figure 5.1 A schematic detailing the various volume fractions simulated to assess the effect of volume fraction on fire resistance**

## 5.2 Analysis Procedure

For this investigation, the thickness of the CRC region will remain fixed at 2 cm but the number of rubber particles will be gradually reduced to simulate a drop in CR volume fraction. In theory, by removing CR particles, space is generated to accommodate the addition of fine aggregates into the concrete mix. It should be noted that the effects of the fine aggregate on the thermal and structural properties of concrete will not be taken into account in this simulation. To this point, the CR volume fraction has been fixed at rough 40%. For the following simulations, the volume fraction will vary from 40% to 10% and then compared to the control case (0% volume fraction).

This will be simulated by randomly removing rubber particles from the previous model to simulate a semi-random distribution that would be expected in a practical application. It is predicted that as the CR volume fraction is reduced, the improvement in failure time will reduce linearly. Physically this is realized because as the volume fraction is reduced, the number of available CR particles to absorb the thermal energy is reduced thus allowing the concrete to heat up faster. The test cases and their associated failure times are shown in Table 5.1 and it was observed that for every 10% reduction in volume fraction, the failure time reduced by roughly 3-5% as expected.

**Table 5.1**
**Test Cases and Failure Times for Various Volume Fractions**

| Cases | CR Volume Fraction | Approximate Failure Time [hrs.] |
|---|---|---|
| **Control Case** | 0% | 3.627 |
| **Case #1** | 10% | 3.743 |
| **Case #2** | 20% | 3.944 |
| **Case #3** | 30% | 4.073 |
| **Case #4** | 40% | 4.206 |

## 5.3 The Effects of Crumb Rubber Volume Fraction

The primary variable of interest is the failure time of the column. Thus for each case, the strain at the steel – concrete interface was plotted against the maximum strain for that case, similar to the procedure described in Section 3.4. Then the failure time for each case was determined based on the intersection of the simulated strain and the formulated failure strain as is shown in Figure 5.2. The time on the horizontal axis is based on the simulated time and the vertical axis is the simulated strain at the steel – concrete interface. The dashed lines represent the max failure strain, as a function of time, according to equation (4.14).

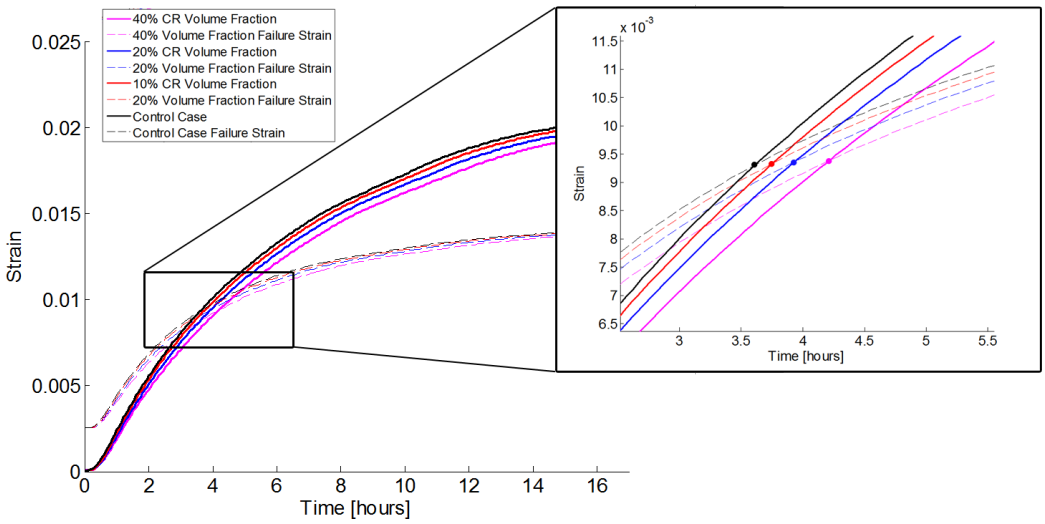


**Figure 5.2 Strain of concrete at steel – concrete interface over the course of the simulation and determination of failure time (inset)**

It can be seen that as the volume fraction is reduced, the time needed for the concrete at the steel – concrete interface to fail is reduced in a nearly linear fashion; this fact is clarified in Figure 5.3. This can be attributed to the fact that as the volume fraction is reduced, there are less rubber particles around to absorb the thermal energy and reduce the propagation of heat within the column. Thus, as predicted, it can be expected that the improvement of the column's fire resistance is directly related to the volume fraction of rubber. To correlate this to a practical application as referenced before, if it is desired to perhaps incorporate a larger aggregate size into the CRC concrete mixture, and in order to maintain the large volume fraction, the thickness of the CRC region would likely need to be increased beyond the 2cm simulated in this study.

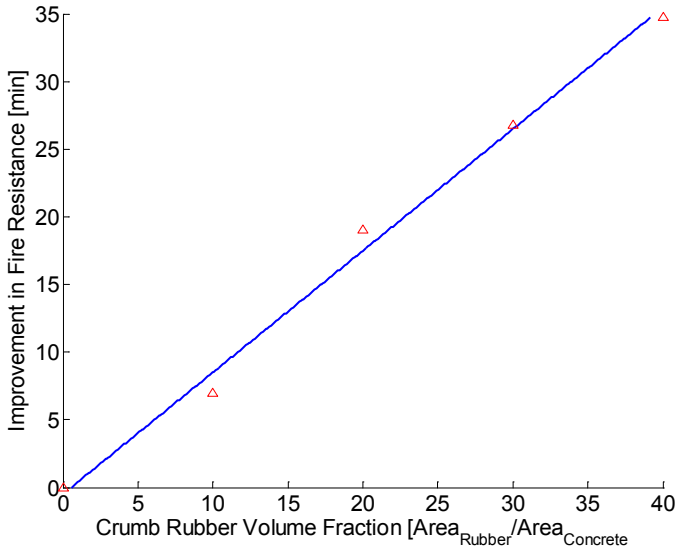


**Figure 5.3 Improvement in Failure Time for Varying Crumb Rubber Volume Fractions**

## 5.4 Summary

The results from the volume fraction simulations verified the initial hypothesis that the improvements in fire resistance were directly related to the volume fraction of crumb rubber used in the insulating region. As stated previously, the simulations in this study fix the thickness of the insulating CRC region to 10% of the radius of the original column, or 2 cm, and as such limits the space for other concrete additives such as aggregates. In the event that larger aggregates are to be incorporated into the cement mixture, a thicker insulating region would need to be considered to allow for a high volume fraction of crumb rubber to be added and still allow for a homogeneous mixture.

# Chapter 6

# SUMMARY AND CONCLUSIONS

## 6.1 Summary of Simulations

Early attempts at improving the performance of concrete has resulted in developing high strength concrete, which exhibits significantly improved properties over normal concrete. One disadvantage is that HS concrete tends to perform poorly in fire situations when compared to normal strength concrete. In order to mitigate this, work has been done to investigate the benefits of addingsteel and polymer fibers, into the HS concrete matrix. These modifications improve the HS concrete by reducing the likelihood and explosive nature of spalling by allowing for channels to be created and release the built up pressure. Further work, specifically targeted towards the fire resistance of reinforced columns, has been geared towards the development of numerical models to help design for improved fire resistance and to predict the onset of failure due to fire. While spalling does pose a danger to personnel, due to its explosive nature, spalling alone does not cause the column to fail, but rather accelerates it by further exposing the reinforcement to fire.

In the first set of analysis in this study, it was determined that the primary cause of failure of a steel reinforced concrete column is the rapid expansion of the steel rebar against the surrounding concrete. This expansion compresses the concrete to the point of failure. This hypothesis was confirmed by running finite element analysis (FEA) simulations under varying conditions, and monitoring when the strain in the concrete at the steel – concrete interface reached the failure

limit. Further simulations were run to investigate the effect of varying the position of the rebar in an attempt to determine a more optimal position. It was found that as the rebar moved closer together, a more catastrophic mode of failure occurred and as the rebar moved further away, i.e. closer to the fire, failure occurred sooner. Thus it was determined that positioning the rebar in the center of the column was ideal. In order to slow the expansion of the steel, and improve the fire resistance of the column, the concept of incorporating a crumb rubber concrete insulating layer was investigated. The fundamental concept of incorporating a CRC region is that the rubber inclusions would absorb some of the thermal energy and thus retard the propagation of heat within the column. As a result the steel would expand slower, thus delaying the onset of failure. This hypothesis was tested through a series of FEA simulations in an effort to quantify the improvement.

The first set of analysis to investigate this concept was done by introducing a region of CRC with a volume fraction of 40%, and whose thickness was 10% of the column's radius. The location of this region was varied within the column, from immediately in front of the rebar and incrementally moving the region towards the edge of the column. It was found that the case where the CRC region was located closest to the rebar (Case #1) performed the best by improving the fire resistance by approximately 45 min; whereas the case of when the CRC region was located at the edge of the column (Case #5) it produced an improvement of approximately 35 min. While in theory Case #1 performed the best, it is practically less feasible since it would require additional casting

processes and also may potentially weaken the overall column due to the lower strength of the crumb rubber concrete. Additionally, Case #1 does not address the issue of spalling since the surface of the column still heats up rapidly. All of these issues were improved in Case #5;nonetheless, an improvement of 35 min is still significant when put into context of a rescue situation.

Lastly, a series of simulations were run to evaluate the effect the crumb rubber's volume fraction has on improvingof the column's fire resistance. It was found that as the volume fraction of crumb rubber was reduced, the improvement in fire resistance also reduced linearly. These results confirmedthe initial hypothesis that as the volume fraction is reduced, the absence of rubber will result in less absorption of the thermal energy and thus the column will heat up quicker. The results also showed that if larger aggregate sizesare to be used in the mixture, the insulating region will need to be larger than the 2cm used in this study. This is because the addition of aggregates will control the amount of rubber and the distribution of rubber within a fixed volume and thus must be taken into consideration.

## 6.2 Conclusions and Recommendations for Future Work

The incorporation of a CRC region to existing or future steel reinforced concrete columns showed great potential for improving their fire resistance. Numerical analysis demonstrated that the rubber inclusions effectively blunt heat transfer within the column, which reduces the rate at which the steel rebar expands; thus increasing the life of the column. FEA simulations run in this study showed improvements of up to 45min;this is approximately a 20% improvement over a

standard SRC column. In addition, there was evidence to suggest that the inclusion of a CRC region on the surface of the column could greatly reduce the potential for explosive spalling by reducing the rate at which the column is heated, as well as introducing channels for the pressure to release through as the rubber degrades.

This study served as the first step in improving the safety of critical load bearing column structures in a fire situation. The results presented in this research encourage future work on experimental testing of the cases presented to both validate the results as well as realistically quantify the improvements. The research contained in this thesis holds both fundamental and experimental applications in the science community as well as the construction industries. These results demonstrate that a simple and environmentally friendly method can easily be incorporated into today's structures in order to effectively increase the fire resistance of concrete columns and lay the groundwork for further experimental research in this area.

# REFERENCES


*Abaqus Version 6.10 Analysis User's Manual.* Providence, RI: Abaqus, 2010.

*Abaqus Version 6.10 Theory Manual*. Providence, RI: Abaqus, 2010.

Almusallam, Abdullah A., Al-Gahtani, Ahmad S., Aziz, Abdur Rauf, and Rasheeduzzafar, "Effect of Reinforcement Corrosion on Bond Strength", Construction and Building Materials. 10 (1996) 123-129.

American Concrete Institute's (ACI) Standard Practice for Selecting Proportions for Normal, Heavyweight, and Mass Concrete (ACI 211.1-91), "*ACI Manual of Concrete Practice 2000, Part 1: Materials and General Properties of Concrete"*. (2000). Print

Anderberg, Y., "Spalling Phenomena of HPC and OC", Proceedings of the International Workshop on Fire Performance of High-Strength Concrete, NIST, Gaithersburg, (1997).

ASCE, "Structural Fire Protection," Manual No. 78, ASCE Committee on Fire Protection, Structural Division, American Society of Civil Engineers, New York, 1992.

Askeland, D. and Phulé, P. *The Science and Engineering of Materials*. 1st ed. Thomson Canada Limited, 2006. Print

Balaguru N, Shah SP. Fiber reinforced cement composites. New York: McGraw-Hill 1992:179–214

Balan, Toader A., Spacone, Enrico., Kwon, Minho. "A 3D hypoelastic model for cyclic analysis of concrete structures" *ASCE Journal of Engineering Structures*. 23(2000), 333-342.

Belyayeva, E.N., and fel'dshtein, M.S. (1973). "The crosslinking, degradation and structural changes during the sulphur vulcanization of isoprene rubbers in the presence of sulphenamides". *Polymer Science. U.S.S.R.* **15**(12), 3055.

Biel, Timothy D., and Lee, H., "Use of Recycled Tire Rubbers in Concrete." *Proceedings of the Third Material Engineering Conference, Infrastructure: New Materials and Methods of Repair*. (1994),351-358,

Cabrita Neves, I., Valentea,J. C., and Correia Rodrigues,J. P. "Thermal restraint and fire resistance of columns". *Journal of Fire Safety*. 37(2002), 753-771.

Collins, Jack A. *Failure of Materials in Mechanical Design: Analysis, Prediction, Prevention.* 2nd ed. John Wiley & Sons, 1993. Print

Colombo, M., di Prisco, M., Felicetti, R., "Mechanical Properties of Steel Fiber Reinforced Concrete Exposed to High Temperatures". Materials and Structures. 43 (2010). 475-491.

Elding Neil N., and Senouci Ahmed B. "Rubber-Tire Particles as Concrete Aggregate". Journal of Materials in Civil Engineering. 5 (1993). 478-496

Eurocode 2, "Design of Concrete Structures. Part 1.2: General Rules—Structural Fire Design (EN1992-1-2)," Commission of European Communities, Brussels, 2004.

Fedroff, D., Ahmad, S., and Savas, B.Z."Freeze-Thaw Durability of Concrete with Ground Waste Tire Rubber*", Transportation Research Record*, 1574(1997), 80-88

Fernández-Berridi,María José, Gonzáleza,Nekane, Mugicaa,Agurtzane and Bernicot,Caroline. "Pyrolysis-FTIR and TGA techniques as tools in the characterization of blends of natural rubber and SBR".*Thermochimica Acta*. 444 (2006), 65-70.

Halasa, Adel F., Prentis, Jim, Hsu, Bill, and Jasiunas, Chad. "High Vinyl High Styrene Solution SBR". *Polymer*. 46(2005). 4166 – 4174.

Hernández-Olivares, F. and Barluenga, G "Fire Performance of Recycled Rubber-Filled High-Strength Concrete". *Cement and Concrete Research*. 34(2004), 109-117

Hernandez-Olivares, F., Barluenga, G., Bollati, M., and Witoszek, B. "Static and Dynamic Behavior of Recycled Tire Rubber-Filled Concrete". Cement and Concrete Research. 32 (2002). 1587-1596.

Hewlett, Peter C. *Lea's Chemistry of Concrete and Cement*, 4th ed. Elsevier, Oxford. (1998). Print.

Jo, B.W., Park, S.K., Park, M.S., "Strength and Hardening Characteristics of Activated Fly Ash Mortars", Magazine of Concrete Research. 59 (2007).

Kaloush, Kamil E., Way, George B., Zhu, Way. "Properties of Crumb Rubber Concrete",*Transportation Research Record: Journal of the Transportation Research Board*. 1914 (2005), 8-14.

Kim, W.I., Kim, S.D., Lee, S.B., and Hong, I.K. (2000). "Kinetic characterization of thermal degradation process for commercial rubbers". *Journal of Industrial Engineering Chemistry, Seoul* **6**(5), 348.

Kodur,Venkatesh. K. R., Dwaikat,M. M. S., and Dwaikat, M. B. "High-Temperature Properties of Concrete for Fire Resistance Modeling of Structures". *ACI Materials*. 105 (2008), 517-527.

Kodur,Venkatesh. K.R., Dwaikat,Mahmud, and Fike,Rustin."High-Temperature Properties of Steel for Fire Resistance Modeling of Structures". *Journal of Materials in Civil Engineering*. 22(2010), 423-434.

Kodur,V. K. R., Wang,T. C., and, Cheng,F. P. "Predicting the fire resistance behavior of high strength concrete columns". Cement and Concrete Composites. 26(2003), 141-153.

Kodur, V.R.; Sultan, M.A., 1998. "Structural Behavior of High Strength Concrete Columns Exposed to Fire" *Proceedings: International Symposium on High Performance and Reactive Powder Concrete*, Vol. 4, 217-232, Sherbrooke, Quebec.

Krishna, R.A., and Pranesh, R.N., Reinforced Concrete Design: Principles and Practice. New Age International Pvt Ltd Publishers, New Delhi (2007). Print.

Lea, F.M. *The Chemistry of Cement & Concrete*, 3rd ed. Edward Arnold, London (1970). Print.

Li, C.Q., Zheng, J.J., Lawanwisut W., Melchers, R.E,. "Concrete Delamination Caused by Steel Reinforcement Corrosion". *ASCE Journal of Materials in Civil Engineering.*19 (2007). 591 – 600.

Li, J., and Hadi, M.N.S., "Behavior of Externally Confined High-Strength Concrete Columns Under Eccentric Loading", Composite Structures. 62 (2003). 145-153.

Li, L., Purkiss J.A. "Stress-Strain Constitutive Equations of Concrete Material at Elevated Temperatures". *Fire Safety Journal* (2005).669-86.

MacNeal, Richard H. "*Finite Elements: Their Design and Performance"* New York: Marcel Dekker Inc., 1995. Print.

Marzouk, H., Hussein, A. "Experimental Investigation on the Behavior of High-Strength Concrete Slabs". *ACI Structural Journal.* 88(1992), 701-714.

Mastral, A.M., Murillo, R., Garcia, T., Navarro, M.V., Callen, M.S., and Lopez, J.M. (2002). "Study of the viability of the process for hydrogen recovery from old tyre oils". *Fuel Process. Technol.* **75**(3), 185.

*NAFEMS A Finite Element Primer*. Glasgow: National Engineering Laboratory, 1992. Print

Nataraja, M.C., Dhang, N., Gupta, A.P., "Stress – Strain curves for steel-reinforced concrete under compression". *Concrete and Cement Composites*. 21 (1999). 383-390.

Nawy, Edward G., Fundamentals of High-Performance Concrete. 2nd ed. John Wiley & Sons, Canada. 2001. Print

Peng, GF., Yang WW., Zhao, J., Liu, YF., Bian SH., and Zhao, LH., "Explosive Spalling and Residual Mechanical Properties of Fiber-Toughened High-Performance Concrete Subjected to High Temperatures" Cement and Concrete Research. 36 (2006). 723 – 727.

Raghavan, D., Huynh, H., and Ferraris, C.F., "Workability, Mechanical Properties, and Chemical Stability of a Recycled Tire Rubber-Filled Cementitous Composite". Journal of Materials Science. 33 (1998). 1745-1752.

Reynolds, C., Steedman, J., Threlfall, A. *Reynolds's Reinforced Concrete Designer's Handbook.* 11th ed. New York: Taylor & Francis. Print

Saafi, M., Toutanji, H.A., and Li, Z., "Behavior of concrete columns confined with fiber reinforced polymer tubes". ACI Materials Journal. 96 4 (1999), pp. 500–509

Sanjayan, G. and Stocks L.J."Spalling of High-Strength Silica Fume Concrete in Fire". ACI Materials Journal. 90 (1993), 170-173.

Schimizze, R.R., Nelson, J.K., Amirkhanian, S.N., & Murden, J.A. "Use of waste rubber in light-duty concrete pavements." *Proceedings of the Third Material Engineering Conference, Infrastructure: New Materials and Methods of Repair*. (1994), 367-374

Sideris, K.K., Manita, P., and Chaniotakis, E., "Performance of Thermally Damaged Fiber Reinforced Concretes", Construction and Building Materials. 23 (2009). 1232-1239.

Song, P.S., Hwang, S., "Mechanical Properties of high-strength steel fiber-reinforced concrete". *Construction of Building Materials*. 18(2004). 669-673.

Su, Z., Microstructure of Polymer Cement Concrete. Delft University Press, Netherlands. (1995). Print.

Thomas, Job, and Ramaswamy, Ananth, "Mechanical Properties of Steel Fiber-Reinforced Concrete", Journal of Materials in Civil Engineering. (2007). 385-392

Taylor, H.F.W. *Cement Chemistry*. 1st ed. Academic Press Limited, London (1990). Print.

Toutanji, H.A., "Use of rubber tire particles in concrete to replace mineral aggregates," *Cement & Concrete Composites*, 18 (1996), 135-139

Underwriters' Laboratories of Canada, Standard Methods of Fire Endurance Tests of Building Construction and Materials". CAN/ULC-S101-M89, Scarborough, Ont., 1989. p. 49

Velez, Mariano. Ceramic and Glass Materials: Structure, Properties and Processing. Springer, (2008). Ch 8. Print.

Xiangjun, D., Yining, D., Tianfeng, W., "Spalling and Mechanical Properties of Fiber Reinforced High-Performance Concrete Subjected to Fire". Journal of Wuhan University of Technology-Materials. (2008).

Youssef, M.A., Moftah,M.,"General stress–strain relationship for concrete at elevated temperatures". *Journal of Engineering Structures*. 29(2007), 2518-2634.

Zaharia, M., Sahajwalla, V., Kim B.C., Khanna, R., Saha-Chaudhury, N., O'Kane, P., Dicker, J., Skidmore, C., and Knights, D., "Recycling of Rubber Tires in Electric Arc Furnace Steelmaking: Simultaneous Combustion of Metallurgic Coke and Rubber Tires Blends" *Energy & Fules*. 23 (2009). 2467-2474.

Zeiml, M., Leithner, D., Lackner, R., and Mang, H.A., "How do Polypropylene Fibers Improve the Spalling Behavior of in-situ Concrete?" Cement and Concrete Research. 36 (2006). 929-942.

# APPENDIX A

# MESH CONVERGENCE TEST RESULTS

The essence of finite element analysis is to model a solid body by discretizing it into a discrete number of finite bodies. To insure that the discretization of the body is sufficient enough to yield accurate results, while maintaining a low computational cost, a mesh convergence study is performed. This study focuses on the region of concrete between the CRC layer and the steel rebar. The meshing strategy used in this research is as follows: the concrete is partitioned into four regions, which is divided along the circumference into 80 elements. This is to ensure that the curvature of the column is well modeled (since 4-node, linear elements are used) as well as ensuring the CRC region is sufficiently meshed. In the radial direction, the length is meshed with 5 different divisions (5, 10, 15, 20, and 30). The region of concrete between the rebar at the center of the column is partitioned with elements of increasing size as accuracy is less important in this region. Lastly, the concrete in the immediate vicinity of the rebar is meshed with an aggressive approach to ensure accuracy and capture the varying contours. This is of increasing importance since failure is determined in this region (Figure A.1).

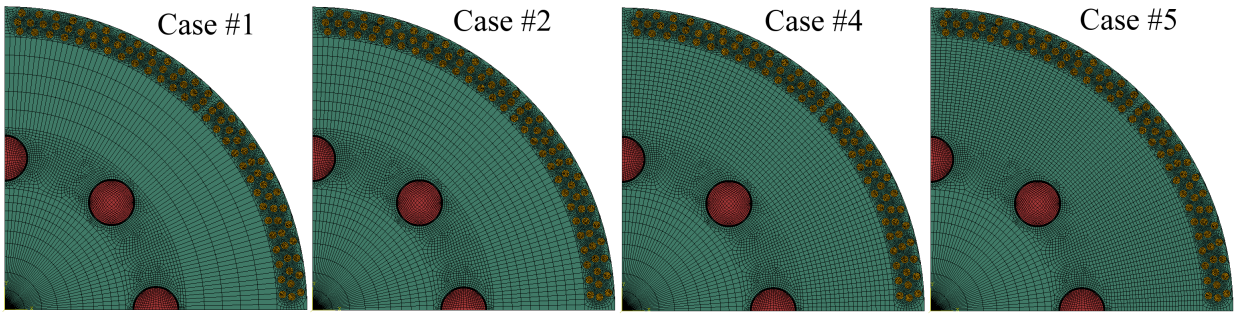


**Figure A.1 Meshing strategy used for convergence testing using CPE4T elements.**

The geometry of the column is 40cm in diameter, and incorporated steel rebar with a diameter of 2.865cm. The CRC region is limited to a thickness of 2cm and the rubber inclusions have a radius of 5mm. The analysis methodology is the same as previously described in the thesis, where the sides of the column are constrained via symmetry conditions and a thermal load is applied to the outside edge of the column. The criterion for determining convergence that will be used is a comparison of strain at several locations of the concrete region.

The results of the mesh convergence study, as can be seen in Figure A.2b, are as expected. With an increasing number of divisions the value of the strain converges to a solution with decreasing error and the results for Case 4 and Case 5 are indiscernible Figure A.2a.

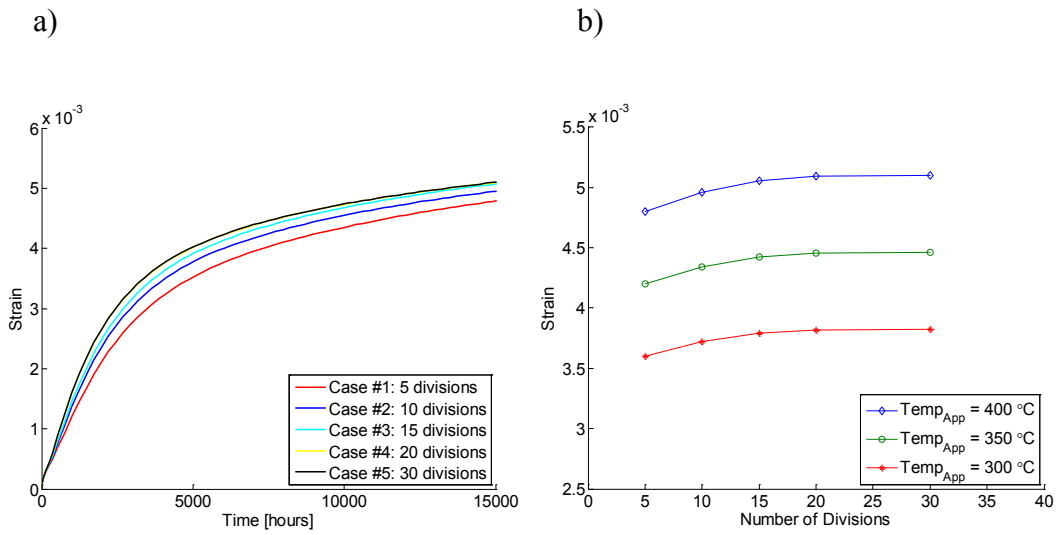


**Figure A.2 Mesh convergence study for (a) strain at the center of the concrete region with negligible difference between the last two cases and (b) analysis of strain at several temperatures as the mesh is refined.**

Furthermore, with an increase in the number of divisions, the percent error in the strain is reduced according to,

$$\%error = \frac{\left|\varepsilon_{I_i}^{n+1} - \varepsilon_{I_i}^{n}\right|}{\varepsilon_{I_i}^{n+1}} \times 100 \tag{A.1}$$

where $\varepsilon_I$ is the max principal strain evaluated at the $i^{th}$ strain for the $n^{th}$ increment in mesh refinement. Based upon the results from the strain in the concrete, an appropriate mesh density with acceptable accuracy for this system is Case 4. The max principal strain is used as a measure in this mesh convergence study since it is the primary indication of failure as indicated by the failure criteria previously discussed. Unless otherwise specified, the geometry and mesh density of Case 4 detailed in this section will be that of the analysis discussed in this thesis.

# APPENDIX B

# CONSTITUTIVE SELATIONSHIPS FOR HIGH TEMPERATURE PROPERTIES OF CONCRETE AND STEEL

**Table B.1**
**Constitutive Relationships for High-Temperature Properties of Concrete**

| | ASCE manual 1992 (NSC) | Kodur et al. 2004 (HSC) |
|---|---|---|
| Stress-strain relationships | $\sigma_c = \begin{cases} f_{c,T}^{'}\left[1-\left(\dfrac{\varepsilon-\varepsilon_{\max,T}}{\varepsilon_{\max,T}}\right)^2\right] & ,\varepsilon \le \varepsilon_{\max,T} \\ f_{c,T}^{'}\left[1-\left(\dfrac{\varepsilon_{\max,T}-\varepsilon}{3\cdot\varepsilon_{\max,T}}\right)^2\right] & \varepsilon > \varepsilon_{\max,T} \end{cases}$ <br> $f_{c,T}^{'} = \begin{cases} f_c^{'} & ,20°C \le T \le 450°C \\ f_c^{'}\left[2.011-2.353\left(\dfrac{T-20}{1000}\right)\right] & ,450°C < T \le 874°C \\ 0 & 874°C < T \end{cases}$ <br> $\varepsilon_{\max,T} = 0.025 + \left(6.0T + 0.04T^2\right)\times 10^{-6}$ | $\sigma_c = \begin{cases} f_{c,T}^{'}\left[1-\left(\dfrac{\varepsilon_{\max,T}-\varepsilon}{\varepsilon_{\max,T}}\right)^H\right] & ,\varepsilon \le \varepsilon_{\max,T} \\ f_{c,T}^{'}\left[1-\left(\dfrac{30(\varepsilon-\varepsilon_{\max,T})}{(130-f_c^{'})\varepsilon_{\max,T}}\right)^2\right] & \varepsilon > \varepsilon_{\max,T} \end{cases}$ <br> $f_{c,T}^{'} = \begin{cases} f_c^{'}[1.0-0.003125(T-20)] & ,T \le 100°C \\ 0.75\times f_c^{'} & ,100°C < T \le 400°C \\ f_c^{'}[1.33-0.00145T] & 400°C < T \end{cases}$ <br> $\varepsilon_{\max,T} = 0.0018 + (6.7f_c^{'} + 6.0T + 0.03T^2)\times 10^{-6}$ <br> $H = 2.28 - 0.012f_c^{'}$ |
| Thermal Capacity | Siliceous aggregate concrete: <br> $\rho c = \begin{cases} 0.005T+1.7 & ,20°C \le T \le 200°C \\ 2.7 & ,200°C < T \le 400°C \\ 0.013T-2.5 & 400°C < T \le 500°C \\ 10.5-0.013T & 500°C < T \le 600°C \\ 2.7 & 600°C < T \end{cases}$ <br> Carbonate aggregate concrete: <br> $\rho c = \begin{cases} 2.566 & ,20°C \le T \le 400°C \\ 0.1765T-68.034 & ,400°C < T \le 410°C \\ 25.00671-0.05043T & 410°C < T \le 445°C \\ 2.566 & 445°C < T \le 500°C \\ 0.01603T-5.44881 & 500°C < T \le 635°C \\ 0.16635T-100.90225 & 635°C < T \le 715°C \\ 176.07343-0.22130T & 715°C < T \le 785°C \\ 2.566 & 785°C < T \end{cases}$ | Siliceous aggregate concrete: <br> $\rho c = \begin{cases} 0.005T+1.7 & ,20°C \le T \le 200°C \\ 2.7 & ,200°C < T \le 400°C \\ 0.013T-2.5 & 400°C < T \le 500°C \\ 10.5-0.013T & 500°C < T \le 600°C \\ 2.7 & 600°C < T \le 623°C \end{cases}$ <br> Carbonate aggregate concrete: <br> $\rho c = \begin{cases} 2.45 & ,20°C \le T \le 400°C \\ 0.026T-12.85 & ,400°C < T \le 475°C \\ 0.0143T-6.295 & 475°C < T \le 650°C \\ 0.1894T-120.11 & 650°C < T \le 735°C \\ -.0263T-212.4 & 735°C < T \le 800°C \\ 2 & 800°C < T \le 1000°C \end{cases}$ |
| Thermal Conductivity | Siliceous aggregate concrete: <br> $k_c = \begin{cases} -0.000625T+1.5 & ,20°C \le T \le 800°C \\ 1.0 & ,800°C < T \end{cases}$ <br> Carbonate aggregate concrete <br> $k_c = \begin{cases} 1.355 & ,20°C \le T \le 293°C \\ -0.001241T+1.7162 & ,293°C < T \end{cases}$ | Siliceous aggregate concrete: <br> $k_c = \{0.85(2-0.0011T) \quad ,20°C \le T \le 1000°C\}$ <br> Carbonate aggregate concrete <br> $k_c = \begin{cases} 0.85(2-0.0013T) & ,20°C \le T \le 300°C \\ 0.85(2.21-0.0002T) & ,300°C < T \end{cases}$ |

$$\frac{E_{c,T}}{E_c} = \begin{cases} 1.0 - 0.0015 \times T, & \text{for } 20°C \le T \le 200°C \\ 0.87 - 0.00084 \times T & \text{for } 200°C \le T \le 700°C \\ 0.28 & \text{for } 700°C \le T \end{cases}$$

*where*,

$E_c$ = Modulus of Elasticity of concrete at 20°C

$E_{c,T}$ = Modulus of Elasticity of concrete at temperature T

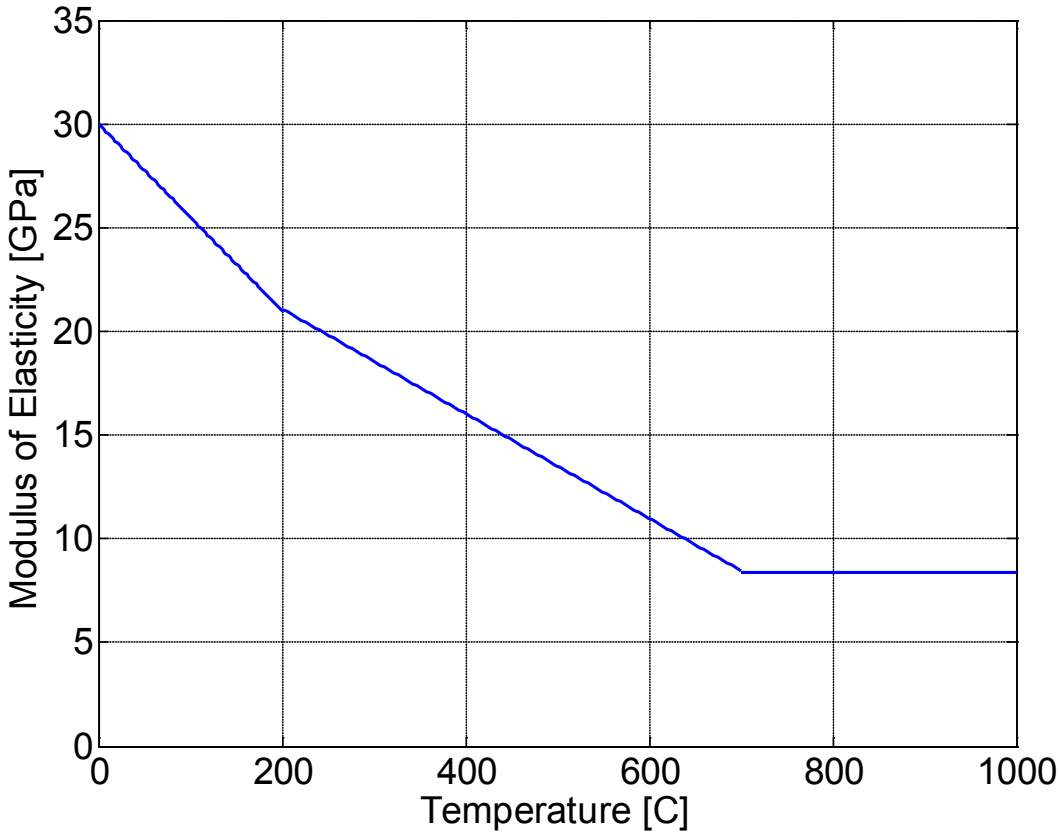


**Figure B.1 Modulus of Elasticity of Concrete at High-Temperatures as Utilized for Modeling in this Study**

$$k_c = \begin{cases} 0.85 \times (2.0 - 0.0013 \times T), & \text{for } 20°C \leq T \leq 300°C \\ 0.85 \times (2.21 - 0.002 \times T), & \text{for } 300°C < T \end{cases}$$

*where*,

$k_c$ = Thermal conductivity of concrete at temperature T

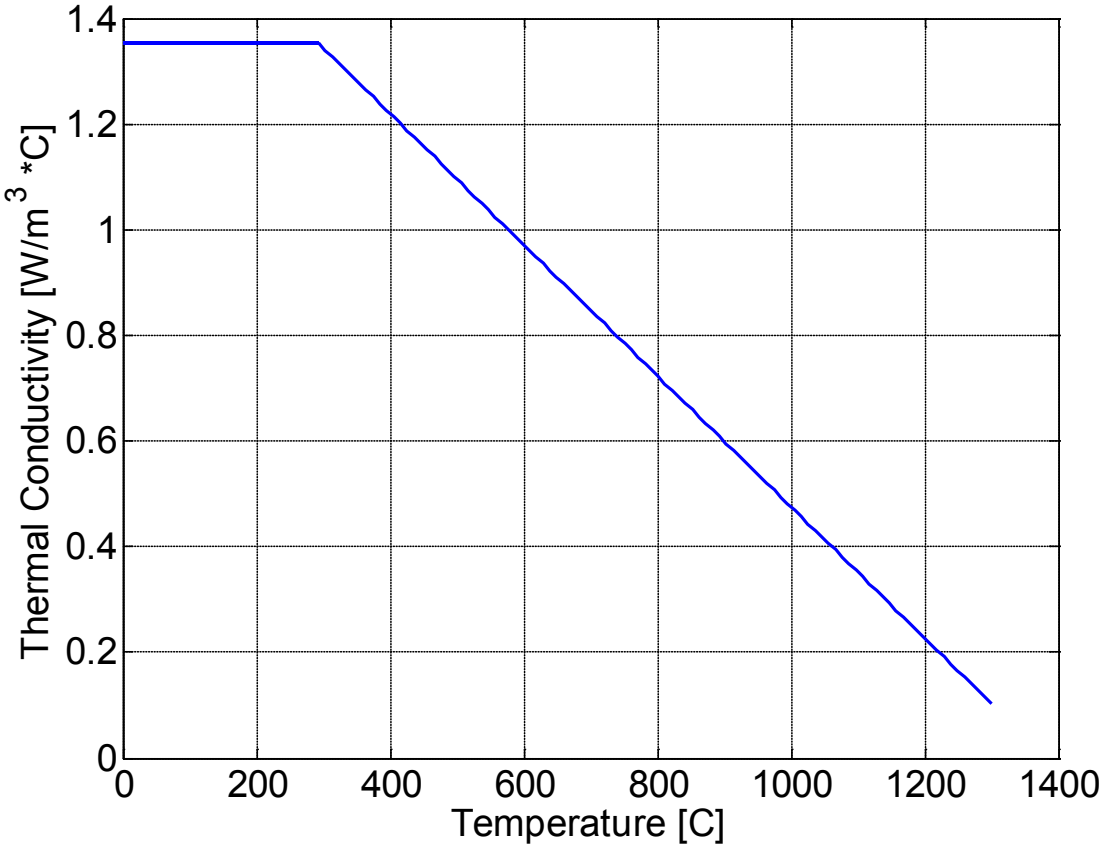


**Figure B.2 Thermal Conductivity of Concrete at High-Temperatures as Utilized for Modeling in this Study**

$$c_c = \begin{cases} 900, & \text{for } 20°C \le T \le 100°C \\ 900 + (T - 100), & \text{for } 100°C \le T \le 200°C \\ 900 + -0.5 \times T, & \text{for } 200°C < T \le 400°C \\ 1100, & \text{for } 400°C < T \le 1200°C \end{cases}$$

*where* :

$c_c$ = specific heat capacity

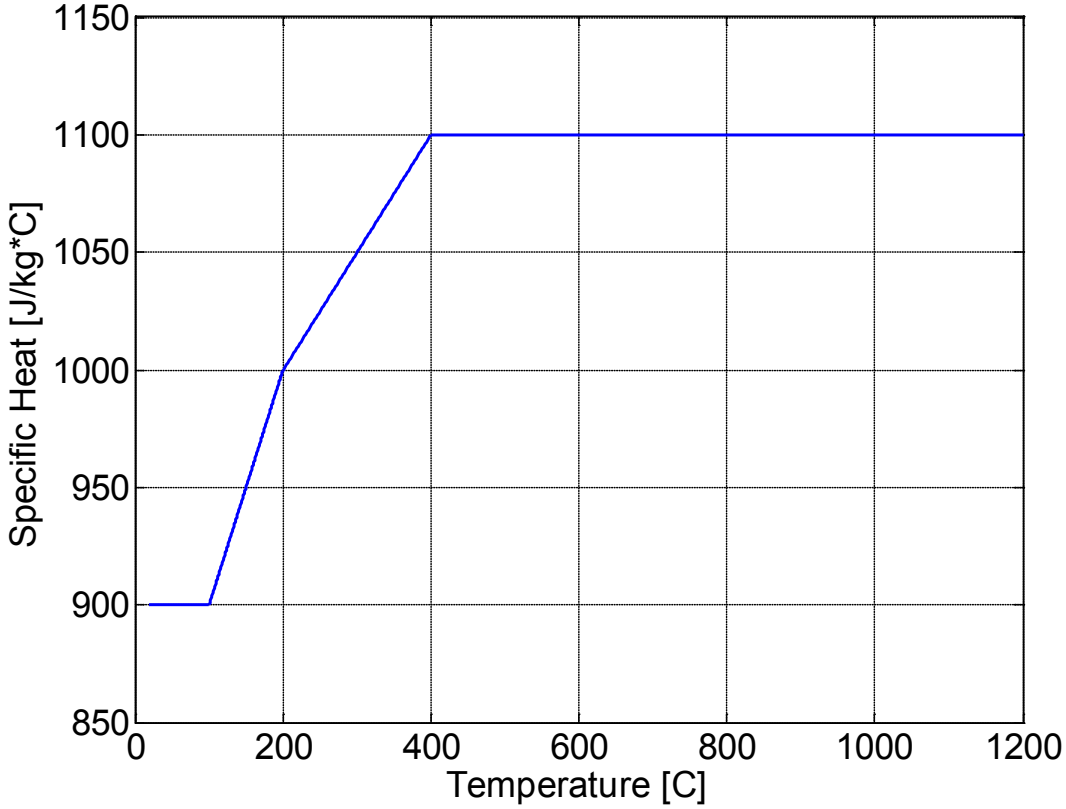


**Figure B.3 Thermal Conductivity of Concrete at High-Temperatures as Utilized for Modeling in this Study**

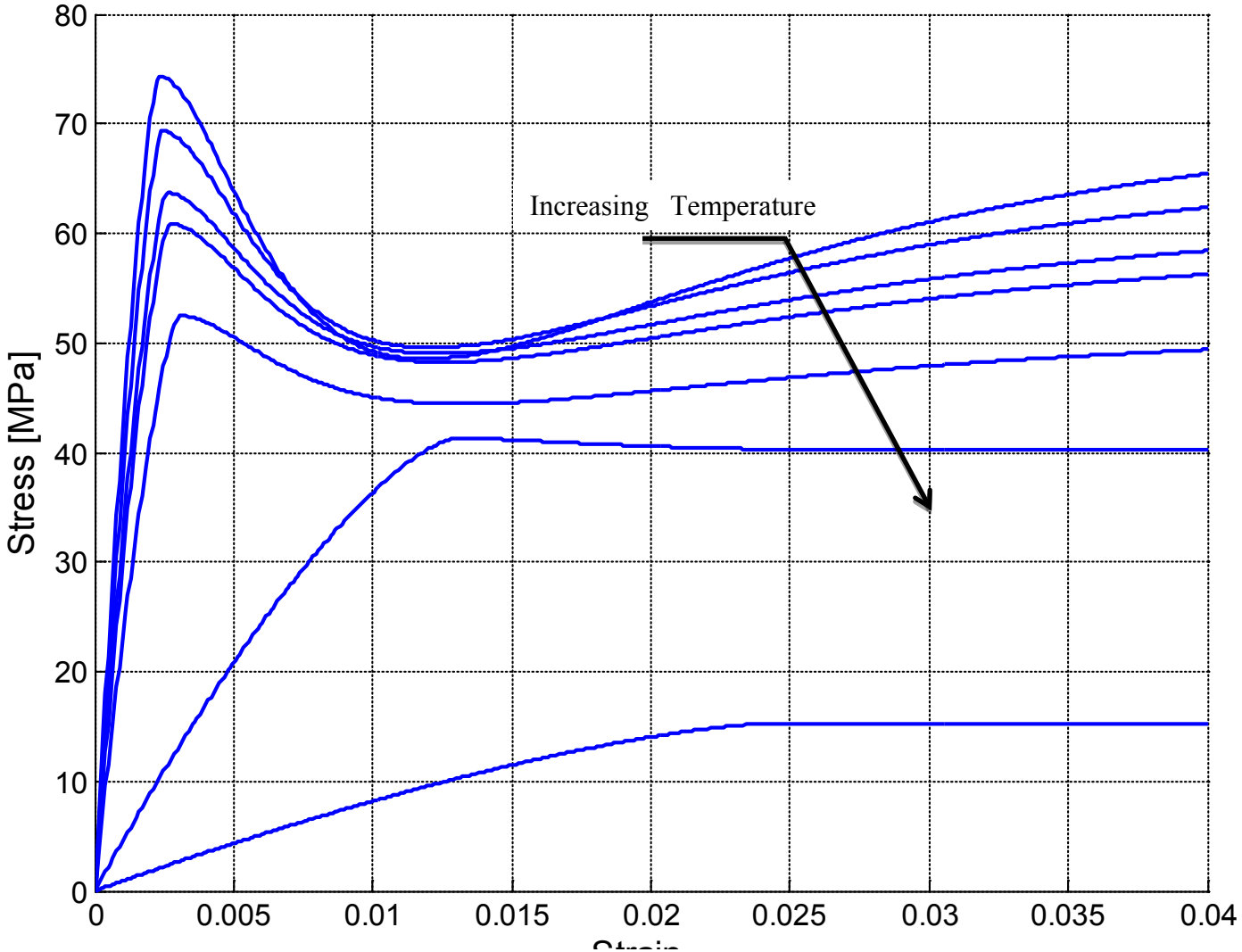


**Figure B.4 Hyperelastic Model of Concrete at High-Temperatures as Utilized for Modeling in this Study**

$$\frac{E_{s,T}}{E_s} = \begin{cases} 1.0 + \dfrac{T}{2{,}000 \ln\left(\dfrac{T}{1{,}100}\right)}, & \text{for } 20°C \le T \le 600°C \\ \dfrac{690 - 0.69T}{T - 53.5} & \text{for } 600°C \le T \end{cases}$$

*where*,

$E_s$ = Modulus of Elasticity of steel at 20°C

$E_{s,T}$ = Modulus of Elasticity of steel at temperature T

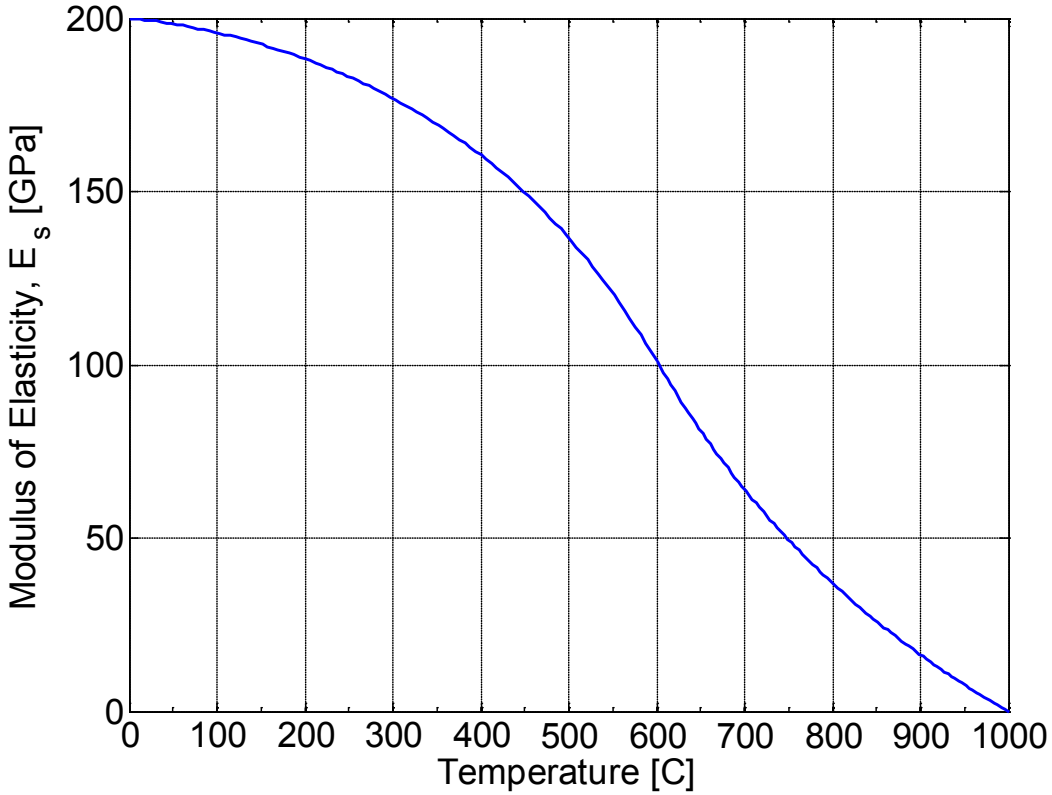


**Figure B.5 Modulus of Elasticity of Steel at High-Temperatures as Utilized for Modeling in this Study**

$$k_s = \begin{cases} -0.022T + 48, & \text{for } 20°C \le T \le 900°C \\ 28.2, & \text{for } 900°C < T \end{cases}$$

*where* :

$k$ = Thermal Conductivity

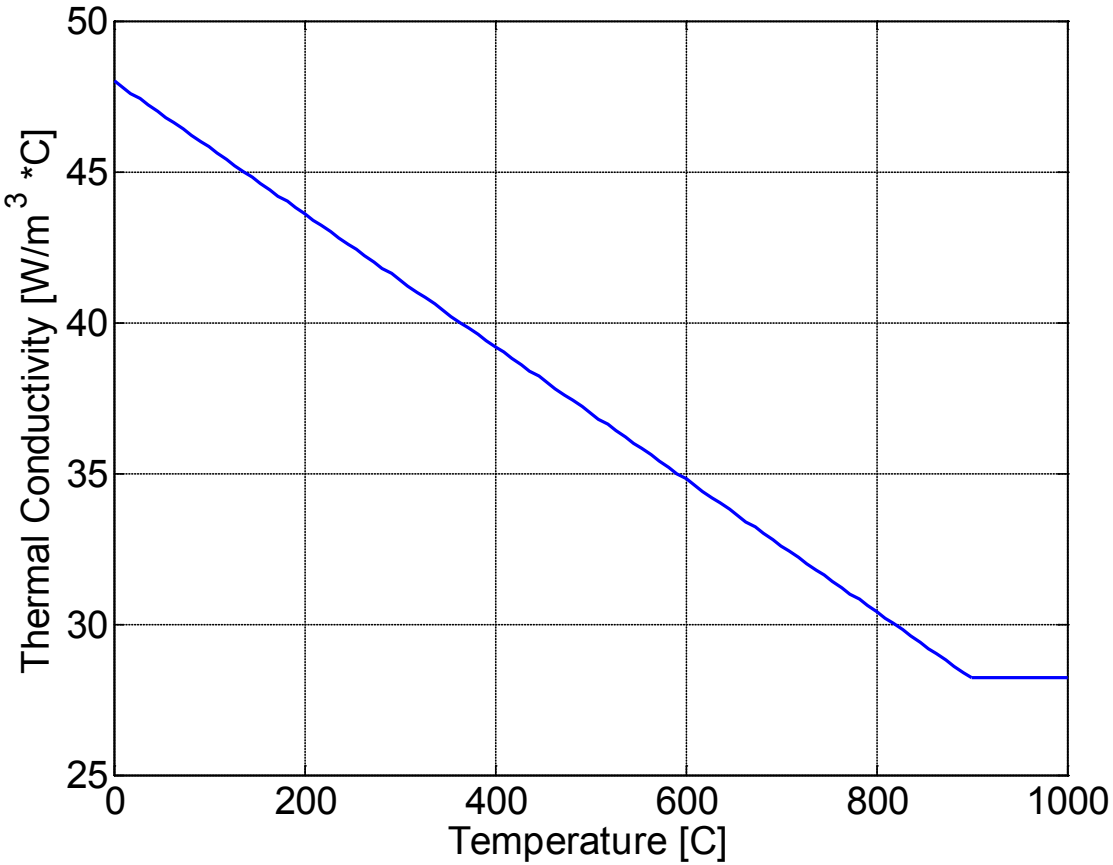


**Figure B.6 Thermal Conductivity of Steel at High-Temperatures as Utilized for Modeling in this Study**

$$\rho_s c_s = \begin{cases} (0.004T + 3.3) \times 10^6, & \text{for } 20°C \le T \le 650°C \\ (0.068T - 38.3) \times 10^6, & \text{for } 650°C \le T \le 725°C \\ (-0.086T + 73.35) \times 10^6, & \text{for } 725°C < T \le 800°C \\ 4.55 \times 10^6, & \text{for } 800°C < T \end{cases}$$

*where* :

$c$ = specific heat capacity

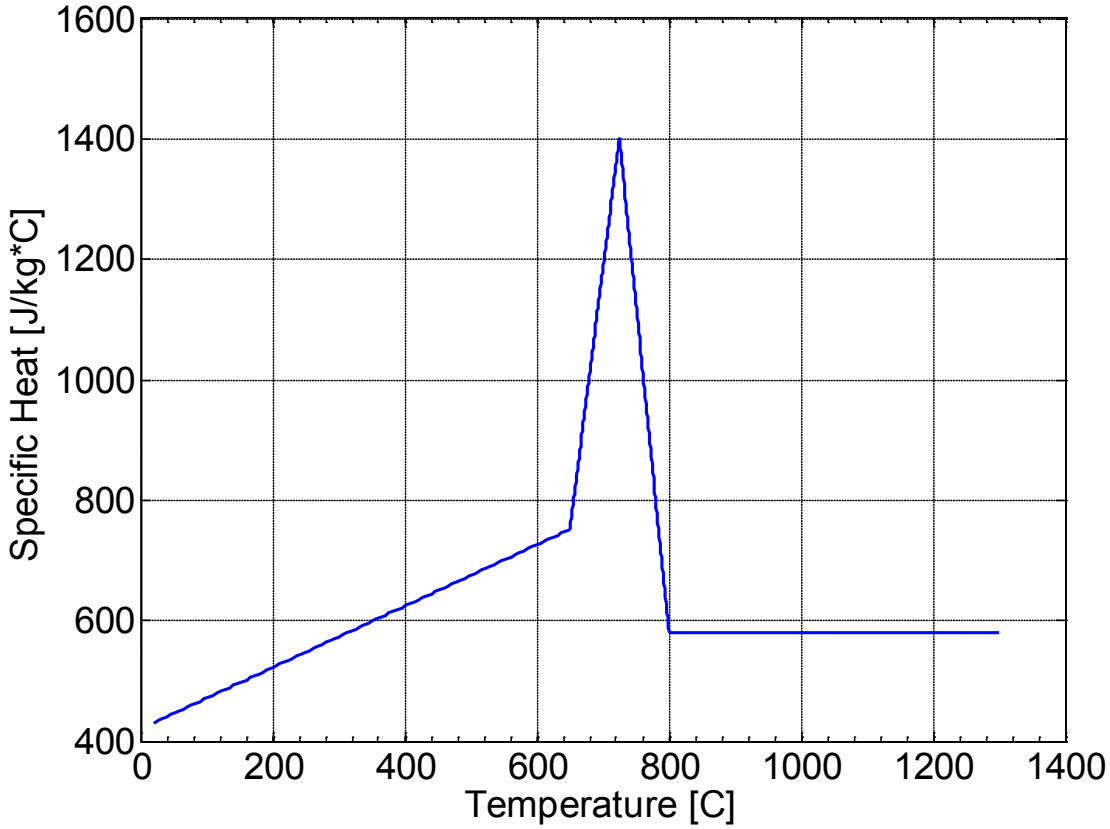


**Figure B.7 Specific Heat Capacity of Steel at High-Temperatures as Utilized for Modeling in this Study**